

MIT LIBRARIES

DUPL



3 9080 02993 0564

V393
.R468

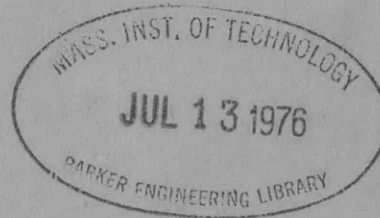
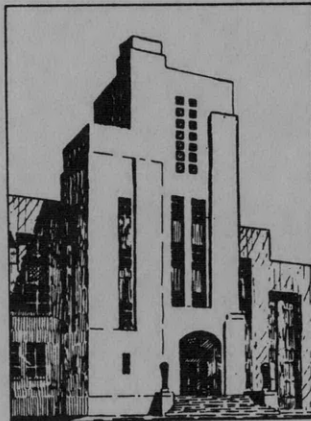
NAVY DEPARTMENT
THE DAVID W. TAYLOR MODEL BASIN
WASHINGTON 7, D.C.

**HYDRODYNAMIC MASSES AND HYDRODYNAMIC
MOMENTS OF INERTIA**

(Hydrodynamische Massen und Hydrodynamische Massenträgheitsmomente)

by

Dr. Eng. Kurt Wendel, Hamburg



Translated by E.N. Labouvie, Ph. D. and Avis Borden, Ph. D.

July 1956

Translation 260

TRANSLATION 260

**This translation to be distributed only
within the continental limits of the United
States and its Territories.**

**HYDRODYNAMIC MASSES AND HYDRODYNAMIC
MOMENTS OF INERTIA**

(Hydrodynamische Massen und Hydrodynamische Massenträgheitsmomente)

by

Dr. Eng. Kurt Wendel, Hamburg

Jahrb. d. STG, Volume 44, 1950

Translated by E.N. Labouvie, Ph. D. and Avis Borden, Ph. D.

July 1956

Translation 260

TABLE OF CONTENTS

	Page
1. Introduction	1
2. Survey of Contents.....	2
I. PRESSURES RESULTING FROM THE ACCELERATED MOTION OF SOLID BODIES IN LIQUIDS. DEFINITION OF THE HYDRODYNAMIC MASSES AND MOMENTS OF INERTIA.	3
3. Pressures Produced on the Surrounding Fluid in Steady and Unsteady Translational Motion in the Two-Dimensional Field of Flow. Hydrodynamic Masses.	3
4. Kinetic Energy of the Field of Flow. Determination of the Hydrodynamic Mass and of the Acceleration Pressures from the Kinetic Energy.	7
5. Hydrodynamic and Apparent Moment of Inertia. Pressures Produced in Unsteady Rotational Motion. General Motion of any Arbitrary Solid in an Ideal Fluid.	10
6. Three-Dimensional Flow	13
7. Experimental Determinations of the Hydrodynamic Masses	15
II. HYDRODYNAMIC MASSES	18
8. Methods of Determining the Potential of Two-Dimensional Fields of Flow	18
9. Hydrodynamic Masses Already Determined Analytically	21
10. Hydrodynamic Masses Determined Experimentally by Means of an Electrical Analogue	24
11. Determination of the Hydrodynamic Masses of Rectilinear Cross Sections.....	25
12. The Hydrodynamic Mass for a Rectangular Cross Section Provided with Bilge Keels	36
13. Distribution of the Acceleration Pressures Over Some of the Cross-Sectional Forms Investigated	39
14. Comparison of Results with Experiments	43
III. HYDRODYNAMIC MOMENTS OF INERTIA	45
15. Hydrodynamic Moments of Inertia Already Determined Analytically.....	45
16. Determination of the Hydrodynamic Moments of Inertia of Rectilinear Sections	46
17. Hydrodynamic Moments of Inertia for a Rectangular Section with Bilge Keels.....	49
18. Comparison of Results with Experiments	51

	Page
IV. EFFECTS OF THE FREE SURFACE, LIMITED DEPTH, FREQUENCY, AND MOTION OF ADVANCE ON HYDRODYNAMIC MASS AND HYDRODYNAMIC MOMENT OF INERTIA	53
19. Influence of a Free Surface.....	53
20. Effect of Finite Depth	58
21. Effects of Frequency and Advance	59
V. APPLICATIONS OF THE HYDRODYNAMIC MOMENTS OF INERTIA	61
22. Tabulation of the Available Values. Additional Calculations	61
23. Application to Elastic Oscillations	61
24. Application to Heaving.....	64
25. Application to Theory of Rolling	65
26. Effect of Limited Depth of Water on Rolling Oscillations and on Vertical Flexural Vibrations	71
REFERENCES	73
DISCUSSION.....	75

1. INTRODUCTION

A solid body moving with unsteady motion in an ideal fluid is subject to hydrodynamic pressure forces which are proportional to the instantaneous values of the acceleration. This result of classical hydrodynamics has been verified with good approximation by experimental investigation on real fluids. Thus, in contrast to the case of steady motion where it is well-known that no resistance occurs in an ideal fluid but does occur in a real fluid, in unsteady motion the representation of the flow in an ideal fluid is suitable for evaluating that portion of the hydrodynamic resistance forces which are produced by the acceleration of the body in the surrounding medium. In the mathematical treatment of the motion of ships these forces have long been associated with a "covibrating water mass"* and an "apparent" moment of inertia. The motion of solid bodies in an ideal fluid was also treated by several theoretical physicists during the second half of the past century; the well-known textbooks of Lamb, Wien, Prandtl-Tietjens, and Durand,^{1,2,3,5} in addition to fundamental concepts, also contain a good deal of information about the numerical evaluation of that component of resistance which must be added in the case of accelerated motion of simple bodies. It is also to be expected that future developments in ship theory will pay much greater attention to the phenomena of nonuniform motion not only as applied to all kinds of vibrations, but also to phenomena of starting and stopping as well as to phenomena associated with steering and course-keeping. Although some of these phenomena, such as the rolling, heaving and pitching motions in calm water as well as the phenomenon of steering, have been considered to be a part of the ship theory ever since the days of Euler, it is nevertheless true that until recently only the dynamic aspect of these problems has been subjected to a more thoroughgoing investigation. The bodies used to be considered as if they were moving in a vacuum except that buoyancy forces were included; the hydrodynamic aspect, however, i.e., the determination of the forces produced by the motion in the surrounding fluid, was given but scant consideration. This was due, on the one hand, to the difficulty of treating mathematically the motion in a real fluid, and on the other hand, to the fact that in the beginning research was concerned with only a qualitative knowledge of the phenomena which could be obtained in a satisfactory manner without determining the hydrodynamic forces or else by determining them only very approximately. If, however, the motion is to be predetermined as accurately as possible, then a precise evaluation of all the forces present, including the hydrodynamic forces, is required. As regards the problems of the ship theory which are to be discussed hereafter, it should also be noted that the hydrodynamic forces due to acceleration are of the same order of magnitude as the inertia forces of the solid bodies which participate in the motion.

*Translator's Note: "Mitschwingende Wassermasse," literally "covibrating water mass"; this is the idealized mass of water which takes part in the motion of the body.

¹References are listed on page 73.

In regard to the designations chosen let us point out the following: In mathematical hydrodynamics, it is perfectly correct to say that the entire effect produced by the presence of the fluid may be represented by a mass which is to be added to the mass of the moving body (Lamb, Art. 68). In contrast to this, we find that in ship theory even to this day the idea has been advocated that the experimentally determined mass increase represents the mass of that volume of water which actually takes part in the motion of the ship. Such a limited volume of water which takes part in the ship's motion does not exist, however. For the purpose of carrying out calculations, it is nevertheless advisable to introduce a fictitious mass as well as a fictitious moment of inertia. In any event, we shall proceed in such manner and we shall designate these quantities as hydrodynamic masses and hydrodynamic moments of inertia. In experimental physics and in English literature on this subject we find that the term "apparent mass" is used instead of hydrodynamic mass;* we shall not follow that example, however, because in ship theory—in Germany at any rate—the designation "apparent mass" (scheinbare Masse) and "apparent moment of inertia" (scheinbares Trägheitsmoment), respectively, have already been generally adopted as expressions for the sum of the mass or the moment of inertia of the solid floating body and any added hydrodynamic mass or moment of inertia, respectively.

2. SURVEY OF CONTENTS

First we shall make a few remarks on the acceleration pressures, especially on their distribution over the surface of the body. In this case as well as later on, our calculations will be confined to the case of two-dimensional flow. The reason for this limitation will be set forth along with the most suitable method of determining approximately the actual case of three-dimensional flow. After examining the experimental results, we shall finally draw conclusions regarding the degree of accuracy of the results obtained analytically.

In the second and third parts, the hydrodynamic masses and moments of inertia will then be determined mathematically for a series of cross sections, especially such sections which resemble the transverse sections of ships. The influence of bilge keels will be discussed in detail. For some of the cross sections investigated the pressure distributions occurring in translation will again be considered. The results will then be compared with the available material.

In Part IV, we then proceed to investigate, likewise by the analytical method, the effects of the free surface and limited depth on the hydrodynamic masses and moments of inertia. Furthermore, the influence of the ship's speed and of the frequency of the oscillation on these quantities will be briefly discussed.

Finally, in Part V, we shall make a few remarks on the application of the hydrodynamic masses and moments of inertia to the theory of elastic oscillations and of rolling and heaving oscillations.

*Translator's note: In English the terms added mass, virtual mass and apparent mass are all used in this connection. Whereas added mass applies only to the hydrodynamic effect there is some ambiguity in the use of the other two terms.

I. PRESSURES RESULTING FROM THE ACCELERATED MOTION OF SOLID BODIES IN LIQUIDS. DEFINITION OF THE HYDRODYNAMIC MASSES AND MOMENTS OF INERTIA

3. PRESSURES PRODUCED ON THE SURROUNDING FLUID IN STEADY AND UNSTEADY TRANSLATIONAL MOTION IN THE TWO-DIMENSIONAL FIELD OF FLOW. HYDRODYNAMIC MASSES.

The velocity potential* for the absolute flow about a cylinder of radius a moving with the velocity U in a fluid which is at rest at infinity is

$$\varphi = -U \frac{a^2}{r} \cos \Theta \quad [1]$$

(Lamb, Art. 68,¹ Prandtl-Tietjens, Art. 78³) where r and Θ are polar coordinates of a coordinate system which has its origin at the center of the cylinder.

In order to set up the relation which correlates the pressures with the velocities, we consider a liquid particle whose center is assumed to lie at the point x, y at the time t . At the time $t + \delta t$, the same particle is located at the point $x + u \cdot \delta t, y + v \cdot \delta t$ where the velocities in the x - and y -directions are designated by u and v . Let us furthermore assume that p represents the pressure, ρ the density, X and Y the components of the external forces per unit mass at the point x, y at the time t , and δx and δy the lengths of the element. In order to be able to use the velocity potential, indicated in Equation [1], which refers to the moving cylinder, we need a system of coordinates which likewise moves with the velocity U of the cylinder. In that case, the change of position of the particle with respect to the moving system is $u - U$ in the x -direction, and after the time δt the velocity components of the particle with respect to this system are

$$\begin{aligned} u + \left[\frac{\partial u}{\partial t} + (u - U) \frac{\partial u}{\partial x} + v \frac{\partial u}{\partial y} \right] \delta t \\ v + \left[\frac{\partial v}{\partial t} + (u - U) \frac{\partial v}{\partial x} + v \frac{\partial v}{\partial y} \right] \delta t \end{aligned}$$

where the brackets represent the acceleration components. (In this case, $\partial u / \partial t$ is to be taken with respect to the moving system.) If we now apply the dynamic law to the particle, with

$$\begin{aligned} \rho \delta x \delta y X \dots \text{ as external force,} \\ \left(p - \frac{1}{2} \frac{\partial p}{\partial x} \delta x \right) \delta y - \left(p + \frac{1}{2} \frac{\partial p}{\partial x} \delta x \right) \delta y = - \frac{\partial p}{\partial x} \delta x \delta y \end{aligned}$$

as the difference of the forces acting on the two end faces, and with

*From the "velocity potential" or "flow potential" of a motion of the frictionless liquid the flow velocity in any given direction is to be determined by differentiating in this particular direction. The velocity component in the x -direction, for instance, is $u = \partial \phi / \partial x$, that in the y -direction is $v = \partial \phi / \partial y$. For further details see References 1 and 3.

$$\rho \delta x \delta y \left[\frac{\partial u}{\partial t} + (u - U) \frac{\partial u}{\partial x} + v \frac{\partial u}{\partial y} \right]$$

as the mass times the acceleration we obtain the equation

$$\rho \delta x \delta y \left[\frac{\partial u}{\partial t} + (u - U) \frac{\partial u}{\partial x} + v \frac{\partial u}{\partial y} \right] = \rho \delta x \delta y X - \delta x \delta y \frac{\partial p}{\partial x}$$

and a symmetrical relation for the y -direction. Simplifying we get

$$\begin{aligned} \frac{\partial u}{\partial t} + (u - U) \frac{\partial u}{\partial x} + v \frac{\partial u}{\partial y} &= X - \frac{1}{\rho} \frac{\partial p}{\partial x} \\ \frac{\partial v}{\partial t} + (u - U) \frac{\partial v}{\partial x} + v \frac{\partial v}{\partial y} &= Y - \frac{1}{\rho} \frac{\partial p}{\partial y} \end{aligned} \quad [2]$$

which are Euler's equations referred to a coordinate system moving in translation with velocity U .

The assumed ideal fluid has a velocity potential; hence, the following applies

$$u = \frac{\partial \varphi}{\partial x} \text{ and } v = \frac{\partial \varphi}{\partial y} \text{ and thus also } \frac{\partial u}{\partial y} = \frac{\partial^2 \varphi}{\partial x \partial y} \text{ and } \frac{\partial v}{\partial x} = \frac{\partial^2 \varphi}{\partial x \partial y}, \text{ hence } \frac{\partial u}{\partial y} = \frac{\partial v}{\partial x}$$

The external forces (the forces of gravity, for instance) and the hydrostatic forces (buoyancy) neutralize each other and need not be considered any further in the investigations to be undertaken which concern only the dynamic forces. If we now introduce these relations into Euler's equations [2], we get

$$\begin{aligned} \frac{\partial^2 \varphi}{\partial x \partial t} + (u - U) \frac{\partial u}{\partial x} + v \frac{\partial v}{\partial x} &= - \frac{1}{\rho} \frac{\partial p}{\partial x} \\ \frac{\partial^2 \varphi}{\partial y \partial t} + (u - U) \frac{\partial u}{\partial y} + v \frac{\partial v}{\partial y} &= - \frac{1}{\rho} \frac{\partial p}{\partial y} \end{aligned}$$

For the purpose of integration, it should be noted that because

$$\frac{1}{2} \frac{\partial}{\partial x} (u)^2 = \frac{1}{2} \frac{\partial}{\partial u} (u)^2 \frac{\partial u}{\partial x} = \frac{1}{2} \cdot 2u \cdot \frac{\partial u}{\partial x} = u \frac{\partial u}{\partial x}$$

the equations may be written as follows:

$$\begin{aligned} \frac{\partial}{\partial x} \left[\frac{\partial \varphi}{\partial t} + \frac{1}{2} (u^2 + v^2) - Uu \right] &= \frac{\partial}{\partial x} \left(- \frac{p}{\rho} \right) \\ \frac{\partial}{\partial y} \left[\frac{\partial \varphi}{\partial t} + \frac{1}{2} (u^2 + v^2) - Uu \right] &= \frac{\partial}{\partial y} \left(- \frac{p}{\rho} \right) \end{aligned}$$

Multiplying by δx and δy , respectively, and performing the integration, we obtain from each one of these two relations

$$\frac{\partial \varphi}{\partial t} + \frac{1}{2} (u^2 + v^2) - Uu + \frac{p}{\rho} = F(t) \quad [3]$$

where the integration constant may still be a function of t . Equation [3] may be designated as a general Bernoulli equation for a coordinate system moving with the velocity U .

We now return to the flow about the cylinder moving with unsteady motion and for this purpose we introduce the velocity potential [1] of the absolute flow in [3] since the flow pattern is carried along with the system. From [1], it follows that

$$\frac{\partial \varphi}{\partial t} = - \frac{dU}{dt} \frac{a^2}{r} \cos \Theta$$

furthermore, since the sum of the squares of the velocity in any two perpendicular directions must always yield the same value

$$u^2 + v^2 = \left(\frac{\partial \varphi}{\partial r} \right)^2 + \left(\frac{\partial \varphi}{r \partial \Theta} \right)^2 = U^2 \frac{a^4}{r^4} (\cos^2 \Theta + \sin^2 \Theta) = U^2 \frac{a^4}{r^4}$$

$$Uu = U \frac{\partial \varphi}{\partial x} = U \left(\frac{\partial \varphi}{\partial r} \cos \Theta - \frac{\partial \varphi}{r \partial \Theta} \sin \Theta \right) = U^2 \frac{a^2}{r^2} \cos 2 \Theta$$

With these expressions we obtain from [3] the following pressure equation for the field of flow about the cylinder:

$$- \frac{dU}{dt} \frac{a^2}{r} \cos \Theta + \frac{1}{2} U^2 \frac{a^4}{r^4} - U^2 \frac{a^2}{r^2} \cos 2 \Theta + \frac{p}{\rho} = F(t)$$

$F(t)$ must be a constant in the present case since the fluid is at rest at a great distance from the cylinder. Since the pressure at infinity is p_0 , when r increases without limit the constant becomes p_0/ρ . On the surface of the cylinder where $r = a$, the pressures are expressed by the relation

$$p = \rho a \frac{dU}{dt} \cos \Theta - \frac{1}{2} \rho U^2 + \rho U^2 \cos 2 \Theta + p_0 \quad [4]$$

Let us now first consider the case of a cylinder moving with uniform velocity. In this case, the acceleration obviously becomes zero and the pressure equation [4] assumes the simple form

$$p = p_0 + \frac{\rho U^2}{2} (1 - 4 \sin^2 \Theta) \quad [5]$$

The pressures remain the same at all times, i.e., the flow is steady. The pressure distribution resulting from [5] can be seen from the plot of the ratio

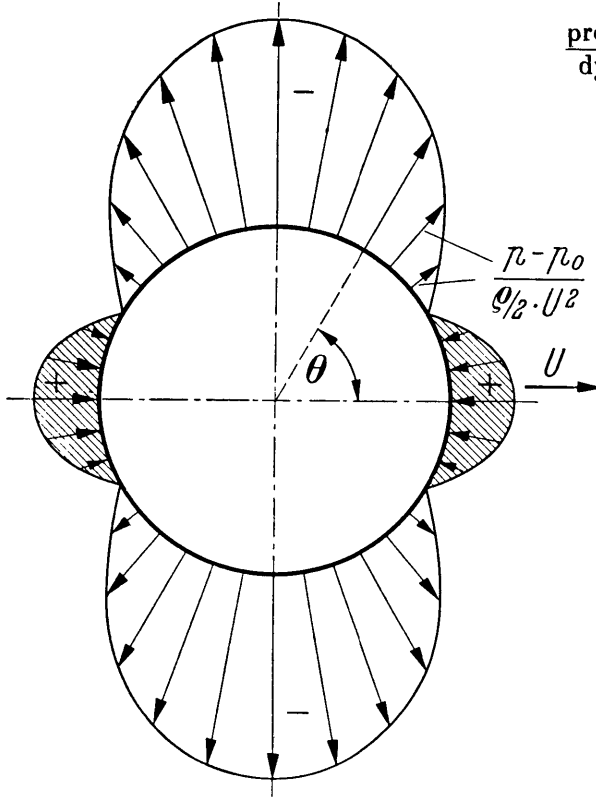


Figure 1 - Pressure Distribution Over the Surface of the Cylinder in Steady Flow
+ Positive Pressure, - Negative Pressure

$$\frac{\text{pressure difference}}{\text{dynamic pressure}} = \frac{p - p_0}{\rho/2 U^2} = 1 - 4 \sin^2 \Theta$$

in Figure 1; we obtain, in particular, for

$$\begin{aligned} \Theta = 0 & \dots \dots \frac{p - p_0}{\rho/2 U^2} = 1 \\ \Theta = 30^\circ & \dots \dots \quad \quad \quad = 0 \\ \Theta = 90^\circ & \dots \dots \quad \quad \quad = -3 \\ \Theta = 180^\circ & \dots \dots \quad \quad \quad = 1 \end{aligned}$$

The resultant pressure disappears; as is well-known no pressure drag occurs in potential flow.

In the case of unsteady motion, however, for which we now proceed to determine the pressure distribution, a pressure resistance does occur, even in potential flow; this we observe right away if we make use of the complete Equation [4]. Now the acceleration is no longer equal to zero and the flow is unsteady. Obviously, the distribution of the pressures resulting from the velocity terms is exactly the same as in the steady case; now, however, the

absolute magnitude of these pressures is no longer constant with respect to the time. Besides, we have to add the pressures resulting from the acceleration term

$$p_B = \rho a \frac{dU}{dt} \cos \Theta \quad [6]$$

whose distribution can be seen from Figure 2. In Figure 2, we have plotted

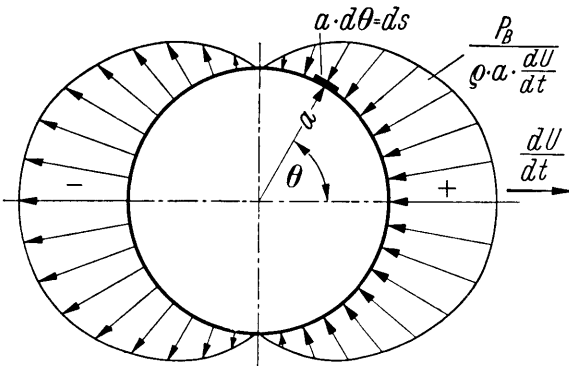


Figure 2 - Acceleration Pressure

$$\frac{p_B}{\rho a \frac{dU}{dt}} = \cos \Theta$$

On the forward face of the accelerated cylinder, which is assumed to be the face toward which the acceleration is directed, the pressure is positive, i.e., it exerts a thrust on the surface of the cylinder while on the opposite face the pressure is negative, i.e., a suction force occurs on the cylinder surface. In contrast to the case of the uniform velocity, the

forces exerted by the fluid pressure on the surface elements of the cylinder do not balance out in this case. They have as a resultant a force acting in a direction opposite to that of the acceleration called the resistance to acceleration. For a unit of length of cylinder the integration results in

$$W'_B = \int_0^{2\pi} p_B a \cos \Theta d\Theta \quad [6a]$$

and with the acceleration pressures given by [6] we have

$$W'_B = \rho a^2 \frac{dU}{dt} \int_0^{2\pi} \cos^2 \Theta d\Theta = \pi \rho a^2 \frac{dU}{dt} \quad [7]$$

Thus, a circular cylinder moving with unsteady motion must overcome this resistance to the acceleration in addition to its own inertial force $m \frac{dU}{dt}$ (m = mass of the cylinder). Expression [7], which must still be multiplied by the length l if the resistance of a cylinder of given length is to be determined, contains a mass

$$m'' = + \pi \rho a^2 l \quad [7a]$$

with an acceleration $\frac{dU}{dt}$. Accordingly, we designate m'' as the hydrodynamic mass of the cylinder in the surrounding fluid. Since the disturbance of the medium extends to infinity, the hydrodynamic mass is not the mass of a particular limited volume of fluid, but is a formal abstraction which adds clarity to the concept.

The total force which must be applied to produce an acceleration of the cylinder thus amounts to

$$W_B = (m + m'') \frac{dU}{dt} = m' \frac{dU}{dt} \quad [8]$$

where m represents the mass of the cylinder, m'' the hydrodynamic mass, and $m' = m + m''$ the apparent mass. The hydrodynamic mass m'' depends only on the size and form and not on the mass of the cylinder. In the case of a circular cylinder—Equation [7a]—the hydrodynamic mass is exactly equal to the mass of the displaced volume of water.

4. KINETIC ENERGY OF THE FIELD OF FLOW. DETERMINATION OF THE HYDRODYNAMIC MASS AND OF THE ACCELERATION PRESSURES FROM THE KINETIC ENERGY.

In the further course of our discussion, we shall not make use of the derivation of the hydrodynamic mass from the general Bernoulli equation. This particular method of determining the hydrodynamic mass was referred to at the outset only because the Euler equations, which express the dynamic law in terms of hydrodynamics, afford an opportunity of giving as clear a representation as possible of the acceleration resistance and hydrodynamic mass. If,

however, easily understandable and simple calculations are to be sought for more complicated cross sections, it is more expedient to determine the hydrodynamic mass from the energy of the field of flow. We shall demonstrate this method also by using the circular cylinder as an example.

The kinetic energy of a flow is given by the expression

$$2 T = -\rho \int_S \varphi \frac{\partial \varphi}{\partial n} ds \quad [9]$$

(see Lamb, Art. 44) when potential flow is involved. The integral is taken over the boundary S of the region occupied by the fluid (two-dimensional flow). T represents the kinetic energy, ρ the density, ϕ the velocity potential, $\partial\phi/\partial n$ the velocity along the normal to the boundary directed into the fluid. Since

$$\frac{\partial \varphi}{\partial n} = \frac{\partial \psi}{\partial s}$$

Equation [9] may also be written* in the form

$$2 T = -\rho \int \varphi d\psi \quad [10]$$

Equations [9] and [10] give the kinetic energy as a function of the velocity potential and of the density ρ . If we succeed in setting up the potential expression for the accelerated body, we can calculate the kinetic energy from [9] or [10]. As far as our use of Equations [9] and [10] is concerned, it should be emphasized that these equations remain valid even for the unbounded fluid regions which are at rest at infinity (Lamb, Art. 46).

For the kinetic energy of the field of flow we may also write $2 T = m'' U^2$; if we substitute the velocity of the body for U in this equation, we get

$$m'' = \frac{-\rho \int \varphi \frac{\partial \varphi}{\partial n} ds}{U^2}. \quad [11]$$

We shall now apply this relation to the circular cylinder and in doing so find that the fictitious mass m'' is the hydrodynamic mass m'' introduced in Equation [7a] above. The potential of the absolute motion was

$$\varphi = -\frac{U a^2}{r} \cos \Theta;$$

* ψ is the "stream-function." $\psi = \text{constant}$ gives the stream-lines. For further information with regard to the velocity potential and the stream-function and the representation of potential flows of the two-dimensional motion by an analytical function $F(z)$ of the complex variable $z = x + iy$, see References 1, 2, 3, 4, and 8.

hence we obtain

$$\frac{\partial \varphi}{\partial n} = \frac{\partial \varphi}{\partial r} = \frac{U a^2}{r^2} \cos \Theta$$

and the kinetic energy for the field of flow which is bounded by the circumference of the cylinder but which, apart from that, extends to infinity is found to be

$$2 T = \rho a^2 U^2 \int_0^{2\pi} \cos^2 \Theta d \Theta = \pi \rho a^2 U^2$$

If we substitute this into [11], we get $m'' = \pi \rho a^2$, which is in fact the hydrodynamic mass for the cylinder of unit length.

For a number of problems in the ship theory it is necessary to know the distribution of acceleration pressure over the boundaries of the cross-sectional area. This distribution can also be determined from the energy of the field of flow. For the circular cross section, for instance, we obtain from Equations [6], [6a], and [7]

$$m'' \frac{dU}{dt} = \int_0^{2\pi} p_B a \cos \Theta d \Theta$$

and with $a d \Theta = ds$

$$p_B = \frac{dm''}{ds} \frac{1}{\cos \Theta} \frac{dU}{dt}$$

With m'' from [11] and the potential from [1] we obtain for the pressure

$$p_B = + \rho a \cos \Theta \frac{dU}{dt}$$

which is the same relation which was previously derived directly from the general Bernoulli equation. (See Equation [6].)

For the numerical determination of the hydrodynamic mass of various cross-sectional forms, the inertia coefficients C introduced by Lewis^{6*} can be used to advantage.

$$C = \frac{m''}{m'' \text{ circle}} \quad [12]$$

*In the literature of hydrodynamics (see Lamb¹ and Munk⁹), the inertia coefficient, in contrast to the above expression, is given as

$$k = \frac{\text{kinetic energy/dynamic pressure}}{\text{volume of displaced body}}$$

Moreover, Munk introduces for the numerator of this ratio the designation "volume of the added apparent mass." The inertia coefficient k has certain disadvantages, particularly for two-dimensional flow, in that it becomes infinite for a plate moving against the direction of flow because the denominator vanishes despite the fact that there exists a well defined kinetic energy.

gives the ratio of the hydrodynamic mass of the cylinder of a particular cross section to the hydrodynamic mass of a circular cylinder with the same maximum diameter $2a$ perpendicular to the direction of motion.

5. HYDRODYNAMIC AND APPARENT MOMENT OF INERTIA. PRESSURES PRODUCED IN UNSTEADY ROTATIONAL MOTION. GENERAL MOTION OF ANY ARBITRARY SOLID IN AN IDEAL FLUID.

From the existence of hydrodynamic masses in translational motions, it naturally follows that hydrodynamic moments of inertia occur in rotational motions. These will also be determined from the energy of the field of flow; for this purpose, it is only necessary to introduce the velocity potential of the rotational motion into the relation for the kinetic energy. Let us consider, for instance, the elliptic cylinder already treated by Lamb. We shall introduce:

$$x = a \cos \eta \quad y = b \sin \eta$$

where a and b are the semi-axes of the ellipse and η designates the angle, indicated in Figure 3, which both coordinates have in common. If we then introduce $a = c \cosh \xi$ and $b = c \sinh \xi$ into the expressions for x and y , we obtain

$$\left. \begin{aligned} x &= c \cosh \xi \cos \eta \\ y &= c \sinh \xi \sin \eta \end{aligned} \right\} \begin{aligned} 0 < \xi < \infty \\ 0 < \eta < 2\pi \end{aligned}$$

with the elliptical coordinates ξ and η . From these relations and the familiar equations defining hyperbolic functions (see Hütte, 26th edition, p. 80) it follows that

$$e^{\xi} = \frac{a+b}{c}, \quad e^{-\xi} = \frac{a-b}{c}, \quad c = \sqrt{a^2 - b^2}$$

Thus, for a rotation about the axis of the ellipse with angular velocity ω , the potential (see Lamb, Art. 72) is

$$\varphi = -\frac{1}{4} \omega (a+b)^2 e^{-2\xi} \sin 2\eta \quad [13]$$

and the stream-function

$$\psi = \frac{1}{4} \omega (a+b)^2 e^{-2\xi} \cos 2\eta \quad [14]$$

If we introduce [13] and [14] into relation [10] for the kinetic energy, we obtain

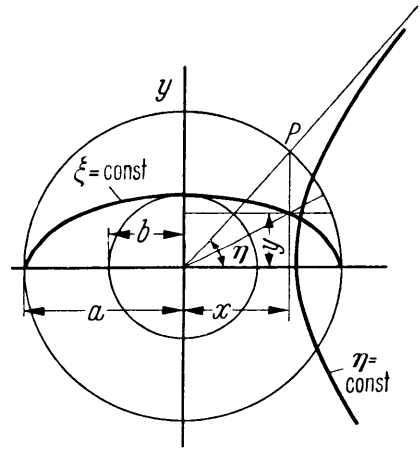


Figure 3 - Elliptic Coordinates

$$2 T = \rho \int_0^{\pi} \frac{1}{8} \omega^2 (a + b)^4 e^{-4 \xi} \sin^2 2 \eta d\eta \quad [15]$$

from which with

$$e^{-4 \xi} = \frac{c^4}{(a + b)^4}$$

we obtain twice the kinetic energy

$$2 T = \frac{1}{8} \pi \rho \omega^2 c^4 \quad [16]$$

This value for the kinetic energy is likewise found in Lamb (see Art. 72). For all confocal ellipses c is constant and likewise the kinetic energy.

Now the following equation holds for the kinetic energy of a rotating solid with the moment of inertia referred to the axis of rotation

$$2 T = J \omega^2$$

If we substitute this relation into Equation [16], we obtain as “hydrodynamic moment of inertia”

$$J'' = \frac{2 T}{\omega^2} = \frac{1}{8} \pi \rho c^4 \quad [17]$$

for a unit length of the rotating cylinder. Therefore, the moment of resistance which in the case of an accelerated rotational motion is to be overcome in an ideal fluid is found to be

$$M_B = (J + J'') \frac{d\omega}{dt} \quad [18]$$

We shall designate $J + J''$ as apparent moment of inertia J' .

It is natural to deduce the distribution of the pressure forces generated by the acceleration $\frac{d\omega}{dt}$ also from the expression for the kinetic energy [15]. From the general definition of the moment of inertia it logically follows that for the hydrodynamic moment of inertia

$$J'' \frac{d\omega}{dt} = -4 \int_0^a p_B y dx + 4 \int_0^b p_B x dy \quad [19]$$

From the equations correlating elliptical and cartesian coordinates it follows that

$$dx = -\frac{ay}{b} d\eta \quad \text{and} \quad dy = \frac{bx}{a} d\eta$$

for fixed ξ ; we naturally assume that particular value of ξ to be chosen which fits the contour of the body. On the other hand, we obtain from [15] and [17]

$$J'' = \frac{2T}{\omega^2} = \frac{1}{8} \rho \int_0^\pi (a+b)^4 e^{-4\xi} \sin^2 2\eta \, d\eta \quad [20]$$

From these two relations [19] and [20] we deduce after a few transformations the desired relation for the pressure distribution

$$p_B = \frac{1}{2} \rho \frac{c^4}{a^3 b^3} x^2 y^2 \frac{d\omega}{dt} \quad [21]$$

For dimensionless plotting it is advantageous to use the expression

$$\frac{p_B}{\rho c^2 \frac{d\omega}{dt}} = \frac{1}{2} \frac{c^2}{a^3 b^3} x^2 y^2. \quad [22]$$

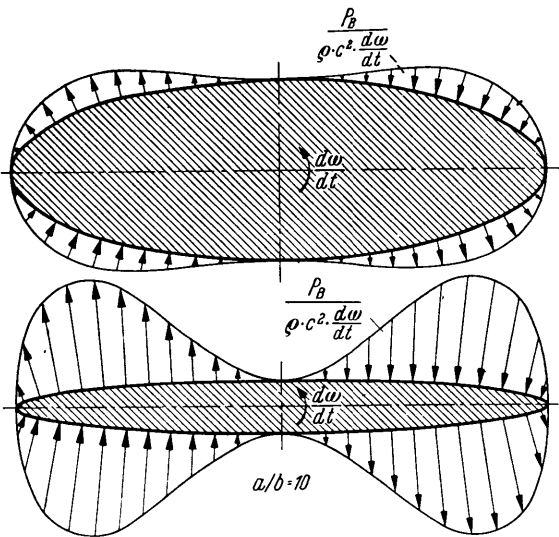


Figure 4 - Pressure Distribution on Rotating Elliptical Cylinders

The pressure distributions calculated in this manner for two different length-width ratios of rotating elliptical cylinders ($a/b = 3$ and 10) have been plotted in Figure 4.

At this point we wish to add a few remarks on the determination of the general motion of a solid of any arbitrary shape in a fluid. Fundamentally, this problem has been solved by Kirchhoff. To recapitulate the extensive and, in part, very complicated line of reasoning of Kirchhoff, who carried out a complete investigation of the ellipsoid, would go beyond the scope of this paper. Hence, we merely call the reader's attention to the treatises of Lamb, Chapter 6,¹ Wiens,² and Munk.⁹ From Kirchhoff's investigation we

merely point out the result that any arbitrary motion of a solid in a surrounding inviscid medium is determined by the velocity components in the direction of the three axes and by the three components of the angular velocity, corresponding to the six degrees of freedom of the general motion, and by the 21 hydrodynamic inertia coefficients. In the most general case, all 21 inertia coefficients are required since in addition to the six squares of velocity, 15 products of velocities must also be inserted into the quadratic expression for the energy. The potential is obtained however by the use of only six terms corresponding to the maximum

number of possible components of motion. From these six expressions in the potential function the inertia coefficients may be calculated. In problems encountered in actual practice, however, such as those posed by stability of course and the steering of airships and ships (see Munk,⁹ Weinblum¹⁰), the flexural vibrations of the ship body (see Lewis,⁶ Koch⁷), the ship oscillations in calm water and in waves (see Brard¹¹), as well as problems which are related to the generation of waves (see Lamb,¹ Havelock¹²), the most general motion is never required; besides, the floating bodies to be considered always contain one or more planes of symmetry so that ordinarily most of the inertia coefficients vanish and thereby simplify the calculations substantially.

6. THREE-DIMENSIONAL FLOW

Analytical investigations treated here will be confined to those processes, such as flow over wings, where the flow is essentially two-dimensional. In practice two-dimensional flow may be realized by mounting the cylindrical body to be investigated in a flow between parallel walls. The situation is different when the calculated inertial coefficients are applied to full-scale conditions. Here bodies are subjected to flows in both longitudinal and transverse or downward directions. If the mathematical calculations are to fit the conditions with reasonable accuracy it is necessary to make an approximate evaluation of the three-dimensionality of the flow as the only practical method for determining the hydrodynamic masses and moments of inertia for hull forms which are not defined by any simple mathematical law. Lewis who was the first to carry out an analytical investigation of the effect of the surrounding medium on the inertial increase for the case of flexural vibrations of ship hulls⁶ has also indicated a method for the approximate evaluation of the tridimensionality. He makes use of the exact solutions derived by Lamb and by himself for the hydrodynamic masses of an ellipsoid of revolution and he defines a longitudinal coefficient of reduction R as follows:

$$R = \frac{\text{actual kinetic energy of the surrounding fluid}}{\text{kinetic energy for the case of two-dimensional flow about the body}}$$

Hence, this coefficient R for the ellipsoid can be calculated with the aid of the exact solution for the latter (Lamb, Art. 114) and with the aid of the kinetic energy for the flow about circular and elliptical cylinders.* This has been carried out by Lewis for the case of the ellipsoid of revolution executing translational oscillations (see Figure 5). Accordingly, for a length/width ratio greater than 6, we have to expect an error of at the most 8 percent if we assume two-dimensional flow about the body. By means of the coefficient of reduction Lewis proceeds to correct the two-dimensional hydrodynamic mass obtained for any arbitrary hull form composed of different transverse sections. It is true that this kind of approximation must be considered

*To this end, the ellipsoid is divided in a longitudinal direction into a number of elementary cylinders. These elements are conceived to be separated from one another by walls across which there is no flow.

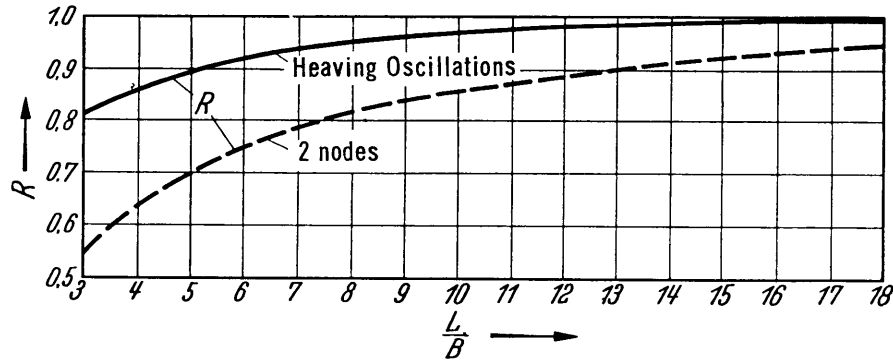


Figure 5 - Coefficients of Reduction According to Lewis

as somewhat rough since it takes into account neither the specific shape of the displacement body nor the width/depth ratio; nevertheless a better approximation which, no doubt, would also be more complicated, seems to be unnecessary as long as we confine ourselves to slender displacement bodies.

Occasionally, the idea is put forth that the hydrodynamic mass and consequently the acceleration pressures of an ellipsoid of revolution moving in translation in a direction perpendicular to its greatest axis must experience a sharp reduction at the ends of the ellipsoid while no reduction at all, or a much slighter reduction, is experienced at the middle. In view of the practical importance of this problem, we shall dwell on this point a little longer. Obviously, if the three-dimensional flow about the body is considered, we obtain, according to Lewis, the same coefficient of reduction over the entire length; hence the same reduction of the hydrodynamic mass results over the entire length. From the analysis of the acceleration pressures it can now be demonstrated that Lewis' method leads to exactly correct results, at least for ellipsoids of revolution. To this end, the acceleration pressures for a special case of the ellipsoid of revolution, viz., the sphere, will be considered. In a manner entirely analogous to that developed in Section 3, wherein the acceleration pressures are found from the general Bernoulli equation in a coordinate system moving with velocity V and by use of the velocity potential of the absolute flow for a circular cylinder in two-dimensional flow, the acceleration pressures on a sphere may be found by extending the relations to three dimensions. A calculation of this kind has been carried out by Prandtl-Tietjens.³ The acceleration pressure on the surface of the sphere is found to be

$$p_B = \frac{1}{2} \rho a \cos \Omega \frac{dU}{dt}$$

where a represents the radius of the sphere and Ω the solid angle indicated in Figure 6.

Accordingly, the pressure at the points A and B on the surface of the sphere (see Figure 6) is

$$p_B = \frac{1}{2} \rho a \frac{dU}{dt}$$

while at corresponding points on a circular cylinder we obtain from Equation [6]

$$p_B = \rho a \frac{dU}{dt}$$

Thus the transformation to three-dimensional flow requires that the equator drawn in the direction of motion from *A* to *B* be reduced by a factor 1/2; this agrees with Lewis' theory which, for the sphere, leads to a coefficient of reduction of 1/2.

It is obvious that this coefficient of reduction must also apply to the two-dimensionally calculated acceleration pressures and likewise to the two-dimensional hydrodynamic masses on all sectional planes drawn parallel to the equator through *A* and *B*; otherwise the hydrodynamic mass for the entire sphere would not be equal to half the mass of the displaced fluid as the calculation (according to Prandtl-Tietjens³) requires.

Besides, Lewis gives solutions for ellipsoids oscillating with one to three nodes which are of interest in connection with flexural vibrations of ship hulls. For these motions coefficients of reduction become smaller with the number of nodes. The curve applying to two nodes is shown as a broken line in Figure 5.

The data of Lewis refer to oscillations and hydrodynamic masses in translation; there is no reason to expect essentially different coefficients of reduction for rotational oscillations about an axis perpendicular to the plane of the two-dimensional motion.

For further information in regard to the three-dimensional treatment of hydrodynamic masses and moments of inertia, we call the reader's attention to the article by Munk in Durand's "Aerodynamic Theory".⁹ In this article, Munk confines himself to the requirements of airship navigation which can also make use of the analysis of ellipsoids because of the generally ellipsoidal shape of airships.

7. EXPERIMENTAL DETERMINATIONS OF THE HYDRODYNAMIC MASSES

Before carrying out the analytical calculation of the hydrodynamic masses and moments of inertia of particular cross sections, we shall first consider whether we expect the theoretical values to agree in general with the empirical values. Such a verification of the calculated values is especially necessary in the field of hydrodynamics since it is well known that a good many of the results obtained on the basis of the assumption of an ideal fluid are in sharp contrast to the processes actually occurring in nature.

In the field of physics, when the sources of error in pendulum observations were investigated, the question first arose as to the manner in which the surrounding air affected the pendulum oscillations. Independently of each other, Dubuat (1786) and Bessel (1826) recognized that the aerodynamic reduction of the length of the pendulum must be carried out by introducing

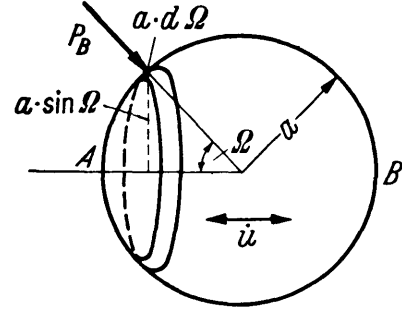


Figure 6 - Acceleration Pressures on the Sphere in Translation

an apparent mass ($m + km'$) instead of the mass of the body of the pendulum m , where m' represents the mass of the displaced air and k is a constant. The value of k for the sphere as determined experimentally by Bessel was found to be ≈ 0.6 . As we have already seen, the theoretical derivation leads to the value of 0.5 [Poisson (1832), Green (1836)]. Taking the internal friction into consideration, Stokes (1856) and O.E. Meyer (1871) later found expressions for k which explained values in excess of 0.5 as resulting from internal friction.* For the special case of a sphere and small oscillations justification was thereby furnished for the agreement between the hydrodynamic mass found experimentally and that derived by calculation.

From an article by L. Schiller, entitled "Impact Tests with Spheres and Disks,"¹³ we mention a few more experimental results regarding the hydrodynamic mass (called "relative apparent mass" by Schiller). In climbing tests with pilot balloons, Hirsch found values which exceed 0.5 only slightly. Cook found the value of 0.46 in an impact test with a mine case in water. Experiments carried out by Lunnon also indicate that the hydrodynamic mass appears to have the same value in a viscous and in an ideal medium, at least in the initial stages of the accelerated motion.

In more recent times, Holstein¹⁴ carried out oscillation tests in water with a parallelepiped. We shall discuss these important experiments in more detail later on in connection with the theoretical calculations. For the time being, we shall merely make use of the value for the hydrodynamic mass of the parallelepiped (width = 12 cm) oscillating at a depth of immersion equal to the half-width. (Two-dimensional flow was obtained by having the lateral walls of the tunnel fit close to the ends of cylinder.) For this case, Holstein finds for the hydrodynamic mass in $\frac{gs^2}{cm}$: $0.0693 < m'' < 0.0805$ with an error of at most $\pm 0.01 \frac{gs^2}{cm}$. The scatter of the m'' values shown by the interval is due to the dependence of the $\frac{gs^2}{cm}$ hydrodynamic mass on frequency. This variation with frequency which occurs in the case of oscillations in or near free surfaces will be discussed in more detail later on. On the basis of a relation derived subsequently (see Part II, Section 11) we obtain by the analytical method for the hydrodynamic mass of a half square parallelepiped: $m'' = 0.0872 \frac{gs^2}{cm}$, i.e., a value which still lies within the limits of error of the experimental determination; in this connection, it should also be kept in mind that Holstein's parallelepiped had slightly rounded edges which must result in a small reduction of the measured hydrodynamic mass, thus rendering the agreement even better.

The test results considered thus far are confined to hydrodynamic masses. Fundamentally, no different behavior is to be expected for the hydrodynamic moments of inertia since they also result from acceleration forces.

*This excess value varies in the case of a sphere with large radius.

Thus we arrive at the result that the hydrodynamic masses and moments of inertia which are determined analytically for a frictionless ideal fluid also satisfy with good approximation at least, the conditions in viscous fluids as long as we are not dealing with very small bodies. Additional test data, especially those obtained experimentally in connection with problems of naval architecture, will be considered in connection with the corresponding results of the analytical calculation.

II. HYDRODYNAMIC MASSES

8. METHODS OF DETERMINING THE POTENTIAL OF TWO-DIMENSIONAL FIELDS OF FLOW

As has been pointed out in Sections 4 and 5, the hydrodynamic masses and moments of inertia can be determined if the velocity potential ϕ on the bounding surface of the respective cross section is known. The theory of the analytical functions provides us with a powerful means for determining the potential of two-dimensional fields of flow.

Every analytical function

$$w = \varphi + i\psi = f(z) = f(x + iy)$$

($\frac{\partial \varphi}{\partial x} = \frac{\partial \psi}{\partial y}$, $\frac{\partial \varphi}{\partial y} = -\frac{\partial \psi}{\partial x}$, Cauchy-Riemann* differential equations) represents a solution of the Laplace equation

$$\Delta w = \frac{\partial^2 w}{\partial x^2} + \frac{\partial^2 w}{\partial y^2} = 0 \quad (\text{Divergence} = 0)$$

furthermore, and like every continuous function of two variables with continuous derivatives, it satisfies the fundamental relation for the existence of a potential

$$\frac{\partial}{\partial y} \left(\frac{\partial w}{\partial x} \right) - \frac{\partial}{\partial x} \left(\frac{\partial w}{\partial y} \right) = 0 \quad (\text{Rotation} = 0)$$

These two conditions are necessary for the existence of irrotational motion in an ideal incompressible medium. ϕ is the velocity potential from which the velocity components at each point of the field of flow $u = \partial\phi/\partial x$, $v = \partial\phi/\partial y$ are to be determined; ψ is the stream-function and $w = \phi + i\psi$ is the complex potential function.

If several potentials exist in a field of flow, they may be superposed as scalar quantities. This linear characteristic is utilized in setting up complicated fields of flow; for example, by superposition of parallel flow and the flow due to a doublet, the field and the potential of the relative flow about the circular cylinder may be found.

Apart from this, the two following methods are primarily used in hydrodynamics to determine the potential:

a. The method of the conformal representation. In this case, one starts out from a known field of flow in the z -plane $\phi + i\psi = f(z) = f(x + iy)$ and maps this conformally into the Z -plane by means of the function f_1 , $Z = X + iY = f_1(z) = f_1(x + iy)$. The new field of flow again represents an analytic function and thereby a possible form of motion. The boundary

*In an analogous manner, these equations also apply for any other two directions which are perpendicular to one another.

of the mapped region ordinarily corresponds to the boundary of the original representation. The infinite character of the field of flow is retained. This method is especially well-known in the field of aerodynamics where it is used to determine the potentials of airfoil sections, for example. For the initial potential function one ordinarily uses the flow about the circle which, in turn, can be determined by a simple transformation ($Z = z + \frac{a^2}{z}$, $a =$ radius of the circle) from the obvious expression for parallel flow $w = -UZ$. (See References 1, 3, 4.)

b. The method of direct solution of the boundary-value problem. Since every analytic function is a solution of the Laplace equation, we only have to find that solution which satisfies the conditions at the boundary of the field of flow (including boundaries extending to infinity). No general methods of solution can be given for the practical solution of this problem. It will be necessary to assume suitable functions and then to find out if they satisfy the required boundary conditions. (A more systematic method is indicated by Lamb,¹ Chapter 4.) In many cases it is possible to first transform, by conformal mapping, the region for which the analytical function is sought into a region in which the boundary conditions are easily satisfied and then to determine the function for the latter region.

We shall illustrate each of the two methods by one example. First, we are going to determine the potential for the circle by the last-mentioned method, i.e., by the direct solution of the boundary-value problem (Lamb, Chapter 4).

Suppose that a cross section in the x -, y -plane moves in the x -direction in a medium which is at rest at infinity. In that case we find that at all points on the contour of the section the velocity component of the fluid in the direction of the normal is equal to the velocity of the boundary in this direction. From this we obtain

$$\psi = Uy + \text{const} \quad [23]$$

as the condition which must be satisfied at the boundary of the section (for more details, see Section 11). At infinity, moreover, the medium must be at rest; therefore, the derivatives of the potential with respect to x and y must vanish there. If we now tentatively substitute $\psi = \frac{A}{r} \sin \Theta$ with r and Θ as polar coordinates into [23], we obtain

$$\frac{A}{r} \sin \Theta = Ur \sin \Theta + \text{const}$$

Moreover, if the expression for x for a radius a is to transform into expression [23], it obviously follows that $\frac{A}{a} = Ua$ and the constant = 0. Thus we find

$$\psi = U \frac{a^2}{r} \sin \Theta$$

and from the Cauchy-Riemann relations

$$\varphi = -U \frac{a^2}{r} \cos \Theta$$

At infinity ($r = \infty$) the derivative of the potential with respect to r vanishes; hence the analytical function $w = \phi + i\psi$ satisfies all boundary conditions. This well-known expression for the potential of the absolute flow about a circular cylinder has already been used several times in Part I.

In an entirely analogous manner Lamb and Durand⁸ determine, with the aid of elliptical coordinates, the potential for an ellipse moving in the direction of the small and large axes.

As a second example, we are going to determine, by the first-mentioned method, i.e., the method of conformal mapping, the potentials for various frame contours from the known potential for the circle. In this case, we follow for the most part the method developed by Lewis.⁶ As transformation function we put $Z = f(z) = z + \frac{b}{z}$. For the circle of unit radius we have $z = x + iy = e^{i\theta}$, for the transformed figure in the Z -plane we have therefore

$$Z = X + iY = e^{i\theta} + b e^{-3i\theta}$$

and since $e^{i\theta} = \cos \Theta + i \sin \Theta$, we obtain thereby

$$\begin{aligned} X &= \cos \Theta + b \cos 3\Theta \\ Y &= \sin \Theta - b \sin 3\Theta \end{aligned} \quad [24]$$

as parametric equations of the transformed figure. For $\Theta = 0$ and $\Theta = \pi/2$, the semi-axes of the figure in the X -, Y -plane are found to be

$$X_1 = 1 + b \quad \text{and} \quad Y_1 = 1 + b$$

By superposition of the parallel flow $w = -Uz$ and the absolute flow about the circle, we obtain for the relative flow about the circular cylinder of unit radius

$$\begin{aligned} \varphi' &= -U \left(r + \frac{1}{r} \right) \cos \Theta \\ \psi' &= -U \left(r - \frac{1}{r} \right) \sin \Theta \end{aligned}$$

and in particular for the boundary $r = 1$

$$\varphi' = 2U \cos \Theta \quad \psi' = 0,$$

which means that the circle is a stream-line. In order to determine the kinetic energy, however, we need to know the absolute flow. Therefore, since the flow at infinity remains unchanged by the transformation, we must again subtract a parallel flow

$w = -UZ = -U(X + iY) = -U[\cos \Theta + b \cos 3\Theta + i(\sin \Theta - b \sin 3\Theta)]$ from the ϕ' and ψ' values of the relative flow which also satisfy the boundary conditions for the transformed circle. Thus we obtain for the absolute flow about the cross section in the Z -plane

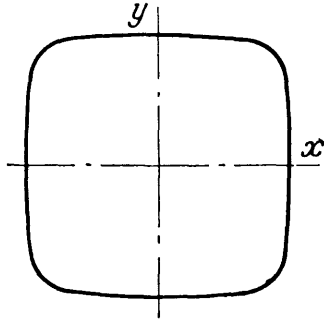


Figure 7 - Transformation
 $Z = z + \frac{b}{z^3}$ of the Unit Circle
 ($b = -0.111$)

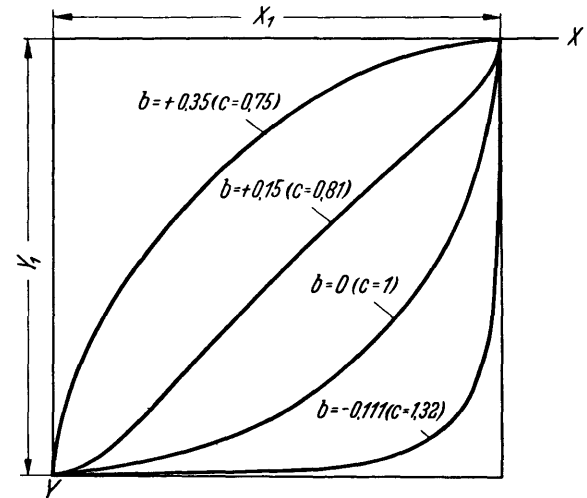


Figure 8 - Transverse Sections Obtained
 from the Conformal Transformation
 $Z = z + \frac{b}{z^3}$ of the Unit Circle

$$\begin{aligned}\varphi &= +U (\cos \Theta - b \cos 3\Theta) \\ \psi &= -U (\sin \Theta - b \sin 3\Theta)\end{aligned}\quad [25]$$

For definite values of b the parametric equations [24] give the transformations of the unit circle into the Z -plane (see Figure 7). For example, we obtain for several values of b the frame sections for which single quadrants are drawn in Figure 8. It is seen that these sections closely resemble normal transverse sections of a ship hull. The constants b are so chosen that the body plan barely lies within the circumscribed rectangle. Lewis⁶ selected the transformation function

$$Z = z + \frac{a}{z} + \frac{b}{z^3}\quad [26]$$

with two undetermined coefficients; he thus succeeded in determining the potentials for a large number of curves like transverse sections which can be varied not only in the curvature, but also in the aspect ratio.

9. HYDRODYNAMIC MASSES ALREADY DETERMINED ANALYTICALLY

Before we turn to the determination of hydrodynamic masses of certain cross sections which are important for naval architecture, we shall discuss a number of hydrodynamic masses already calculated by other authors for such sections that resemble hull cross section.

By introducing the potential of the absolute flow about the circle and the ellipse into

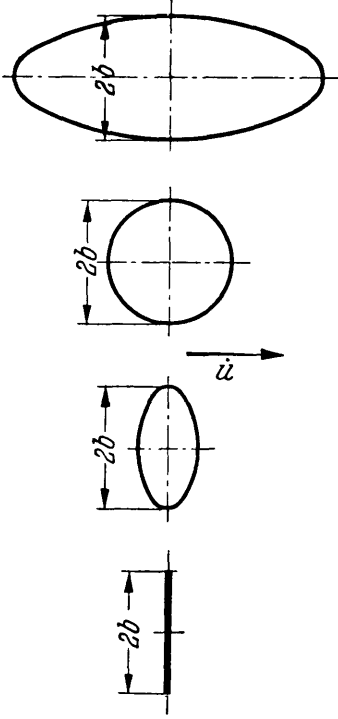


Figure 9 - Ellipses of Different Aspect Ratio but of Equal Hydrodynamic Mass

the relations for the kinetic energy [9] and [10] as derived in Part I, we find the kinetic energy and from this the hydrodynamic mass m'' [11] and the inertia coefficients C [12] for the respective cross section.

For the motion of the ellipse in the direction of the main axis a , we find the hydrodynamic mass to be $\rho \pi b^2$ where b denotes the semi-axis perpendicular to the direction of motion. This expression is independent of the length-width ratio of the ellipse; hence, for all ellipses of equal breadth, which specifically include the circle and the flat plate, the hydrodynamic mass is the same. Obviously, the inertia coefficient C for all cross sections drawn in Figure 9 is equal to 1.

In more recent times, Lewis⁶ determined the potential for forms resembling transverse sections by means of the conformal representation discussed in the preceding section. The kinetic energy for the motion of the sections with the "length-width ratio" $X_1/Y_1 = 1$ is obtained from [25] and [10] as follows:

$$2T = \rho U^2 \int_{2\pi}^0 (\cos \Theta - b \cos 3\Theta) (\cos \Theta - 3b \cos 3\Theta) d\Theta$$

which, after carrying out the integrations, results in

$$2T = \rho \pi U^2 (1 + 3b^2) \quad [27]$$

A circular cross section having the semi-axis $X_1 = Y_1 = 1 + b$ as radius has kinetic energy $2T = \rho \pi U^2 (1 + b)^2$; hence, the inertia coefficient is

$$C = \frac{1 + 3b^2}{(1 + b)^2} \quad [28]$$

and the hydrodynamic mass for such a double-frame profile, moving in the direction of the axes, is

$$m'' = \rho \pi C \left(\frac{B}{2} \right)^2$$

where B represents the greatest width of the profile. Therefore, if we choose definite inertia coefficients C , we can determine from [28] first of all the corresponding b and from [24] the

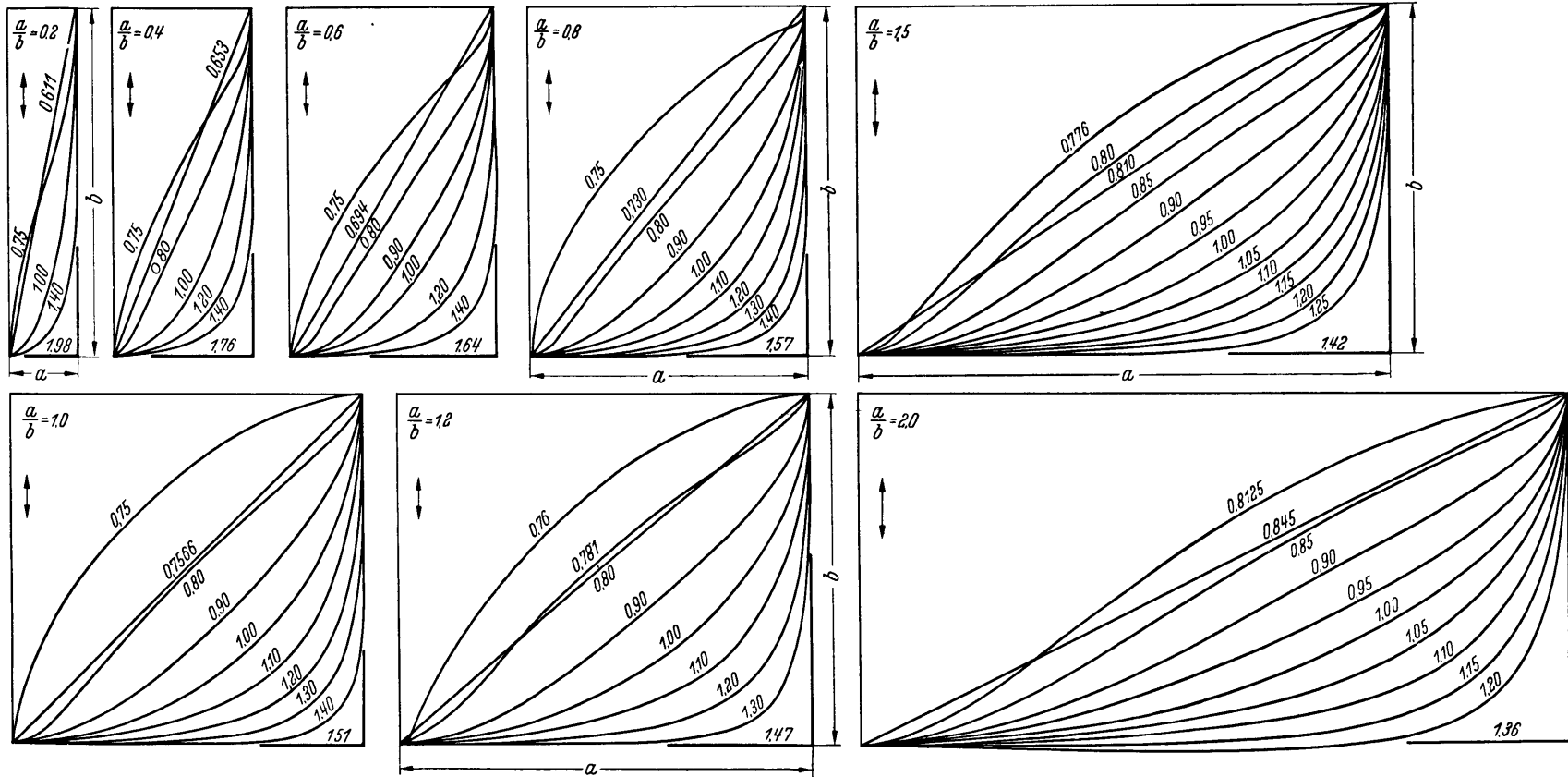


Figure 10 - Transverse Sections and Inertia Coefficients Obtained by Lewis

lengths of the semi-axes and finally the shape of the section. In this manner, using the transformation function [26], Lewis determined the inertia coefficients C for the potentials for sections of various curvature. Lewis's transverse sections, together with the corresponding C -values, are shown in Figure 10. In these figures, the arrow in the upper left corner denotes the direction of translational motion and a/b the length-width ratio of the circumscribed rectangle. (In the figure, one of the semi-axes is designated by b , which is not to be confused with the constant b of the transformation function.)

Lewis determined the hydrodynamic mass not only for curvilinear forms, but also for rectangles and rhombuses of various length-width ratios, by a conformal mapping of the parallel flow into a flow with polygonal boundaries by means of the Schwarz-Christoffel transformation. The values of C obtained in this manner are also given in Figure 10. From these representations we conclude that conditions do not change materially when passing from the full-form transverse section to the rectangle. Hence, as long as we endeavor to determine the hydrodynamic masses and moments of inertia by the analytical method, the error made in replacing the usual full-form transverse sections amidships by rectangles is kept within moderate and approximately specified limits.

10. HYDRODYNAMIC MASSES DETERMINED EXPERIMENTALLY BY MEANS OF AN ELECTRICAL ANALOGUE

The potential V of a plane electric field likewise satisfies the Laplace equation

$$\Delta V = \frac{\partial^2 V}{\partial x^2} + \frac{\partial^2 V}{\partial y^2} = 0$$

Hence, for every mechanical problem which is based upon the equation $\Delta w = 0$, there may be substituted an analogous electrical problem. Koch⁷ has indicated an electrical analogue in the present problem for the determination of the hydrodynamic mass of water. It is essential in this connection that it is possible to realize the electrical analogue experimentally. By purely electrical measurements of resistance, current intensity, and voltage carried out with an electrical circuit, a quantity $\bar{\phi}$ corresponding to the inertia coefficient C can be determined and by means of this quantity the hydrodynamic mass may be represented in the form

$$m'' = 2\rho \bar{\phi} b^2$$

where b denotes half-width of the cross section measured perpendicular to the motion. The quantity $\bar{\phi}$ is equivalent to $\pi/4$ times the inertia coefficient C introduced above, where the procedure outlined by Lewis was followed.

From the standpoint of hydrodynamics, these tests not only simplify the method and reduce the number of calculations but they duplicate almost exactly the conditions in an ideal fluid. Koch investigated the rectangular cross section in a bounded and in an unbounded medium by this method and in doing so, he also represented electrically the effect of the free

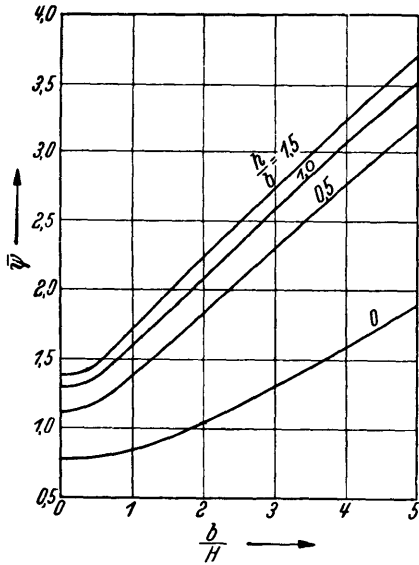


Figure 11 - Inertia Coefficients for Rectangles Obtained by Koch's Electrical Experiments

Motion normal to the free surface.
 H = depth below keel, h = draft,
 b = half-width

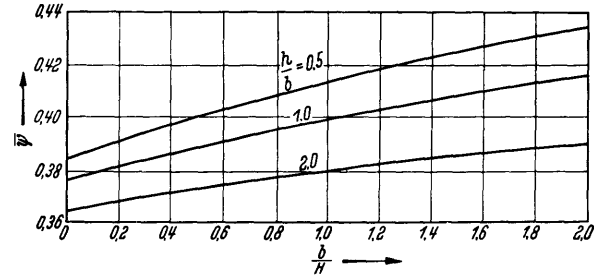


Figure 12 - Inertia Coefficients for Rectangles Obtained by Koch's Electrical Experiments

Motion in the direction of the free surface.
 H = depth below the keel.

surface which is essential in treating transverse oscillations. Figure 11 gives the test results for vertical motions in a direction normal to the free surface ($\bar{\phi}$) while Figure 12 indicates the results for the rectangular cross section moving in the direction of the free surface ($\bar{\psi}$). The parameter h/b denotes the aspect ratio in these figures; b is taken perpendicular to the direction of motion of Figure 11 while in Figure 12 it is taken in the direction of the motion.

11. DETERMINATION OF THE HYDRODYNAMIC MASSES OF RECTILINEAR CROSS SECTIONS

In the preceding sections we have seen that the hydrodynamic masses of a great many cross sections for an unbounded medium have already been determined (ellipses and their related forms, transverse sections, rectangles, and rhombuses). It would be desirable to supplement the results obtained thus far by determining m'' for transverse sections with bilge keels. (The role, which the hydrodynamic masses and the resulting distribution of acceleration pressures associated with them, play in the evaluation of the phenomenon of rolling will be mentioned later on; see Section 23.) Since ships are usually full-formed in the region over the length of the bilge keels, the investigation of the effect of bilge keels was carried out on rectangular cross sections. Furthermore, an essential factor in making this choice was the relative facility with which the calculations for rectilinear cross sections can be carried out; moreover, as in the case of the ellipse, the fact that the entire range of all possible forms is included by the variation of a single parameter, viz., the aspect ratio, combined with the fact just mentioned, make this a desirable choice.

The method selected, which will be applied in an analogous manner to all investigations to be undertaken, will first be demonstrated for the case of a rectangle moving in a direction

parallel to its sides. In this case, we are able to draw a comparison with the calculations carried out in a different manner by Lewis as well as with the experiments undertaken by Koch.

The potential is determined by means of the method of direct solution of the boundary-value problem as described in Section 8b. To do this, we have to transform the field about the rectangular cross section under consideration into simpler regions. For rectilinear cross sections, the theory of functions provides us with a method in the form of the Schwarz-Christoffel theorem by which, among other things, a conformal mapping of the exterior of a polygon into a half-plane is possible (see References 1, 15, 16, 20, and 22).

The function

$$z = f(t) = c \int_0^t (t_1 - t)^{-\frac{\mu_1}{\pi}} (t_2 - t)^{-\frac{\mu_2}{\pi}} \dots (t_n - t)^{-\frac{\mu_n}{\pi}} dt + c' \quad [29]$$

where z and t are complex variables; $t_1, t_2 \dots t_n$, points on the real axis; $\mu_1, \mu_2 \dots \mu_n$, real numbers; and c and c' real or complex constants; represents a transformation of the upper half-plane $t = u + iv$ [$J(t) \geq 0$] into a polygonal region of the $z = x + iy$ -plane. For the mathematical proof of this theorem established by Schwarz-Christoffel, the reader's attention is directed to the bibliographical references cited^{15,16} as well as to the more detailed textbooks of the theory of functions. In our case, we shall confine ourselves to the demonstration of the theorem for those regions which occur in the problems which we endeavor to solve.

Let us consider the shaded region of the z -plane (see Figure 13). By means of the Schwarz-Christoffel formula [29], it is possible to transform the upper half of the t -plane (see Figure 14) into this polygonal region of the z -plane which extends to infinity. In particular, the real axis of the t -plane is to map into the polygonal boundary of the z -plane. The points $t_1 \dots t_n$ correspond to corners of the polygon in the z -plane and the real exponents $\mu_1 \dots \mu_n$ indicate the size of the exterior angles through which each successive side of the

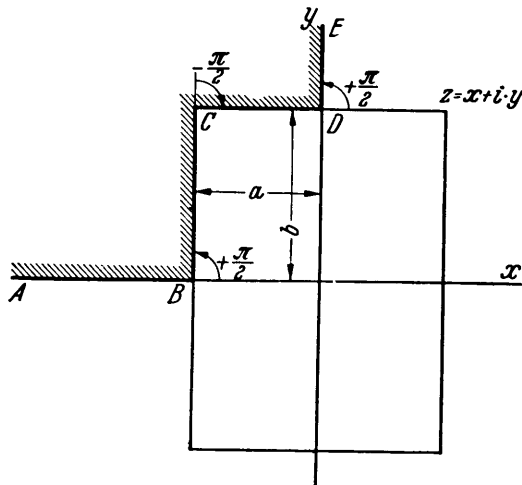


Figure 13 - z -Plane

polygon must be rotated in order to pass continuously to the next side. Into the transformation equation [29] we must therefore introduce the points $t = 0, k$ and 1 for $t_1 \dots t_n$; in addition, the point ∞ of the u -axis should correspond to a corner at $z = \infty$. Finally, the real numbers $\mu_1 \dots \mu_n$ are defined by the exterior angles of

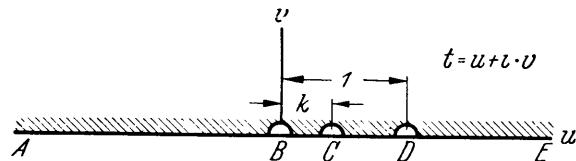


Figure 14 - t -Plane

the polygon (see Figure 13); they are $\mu_1 = +\frac{1}{2}\pi$, $\mu_2 = -\frac{1}{2}\pi$, $\mu_3 = +\frac{1}{2}\pi$ ($\mu > 0$ for angles with positive rotation and $\mu < 0$ for angles with negative rotation). If we take into account this rule of signs, we obtain $\sum_{i=1}^{i=n} \mu_i = 2\pi$, as can easily be verified for simple polygons. In such cases as the one just considered, the polygonal region may extend to infinity; in an analogous manner, for the region between two parallel lines, as shown in Figure 15, the exterior angle π must be introduced into the calculation while for the region extending to infinity as shown in Figure 13, the calculation requires the exterior angle $3/2\pi$. Thereby, the transformation equation becomes

$$z = c \int_0^t (-t)^{-\frac{1}{2}} (k-t)^{\frac{1}{2}} (1-t)^{-\frac{1}{2}} dt + c' \quad [30]$$

and after adding the corner at infinity we obtain for the sum of the exponents μ_i : $\sum \mu_i = 2\pi$, as required; moreover, the constants c and c' permit us to arbitrarily change the position of the representation in the z -plane; we choose its position in such a way that the position of the polygon indicated in Figure 13 is obtained, i.e., the points in the t - and z -planes designated by the same letters are supposed to transform into each other.

We now follow the mapping of the real axis in the t -plane into the z -plane where it is supposed to go over into the boundary of the polygon and thereby the constant is fixed. Starting at $-\infty$ (point A), we first allow t to traverse the u -axis as far as $t = 0$ (point B).



Figure 15

The integrand remains real along the entire path, and z travels from $-\infty$ to $-c'$, thus traversing the segment AB in the z -plane if we set the still undetermined constant

$$c' = -a \quad [31]$$

Over the next portion of the t -axis (segment BC) where $0 < t < k$, the integrand becomes imaginary in the denominator because of the term $\sqrt{-t}$. If we now dispose of c in such a manner that for $t = k$

$$z = c \int_0^k -a = -a + i b$$

applies, or that

$$c = \frac{ib}{k} \quad [32]$$

(the constant is therefore real), then

$$z = ib \frac{0}{k} - a$$

traverses exactly the segment BC in the z -plane. The segment CD in the t -plane is traversed for $k < t < 1$ and for this region we obtain two imaginary roots in the integrand; thus the integrand becomes real and we obtain for $t = 1$

$$z = ib \frac{\int_0^1}{k} - a = \frac{ib}{k} \left(\int_k^1 + \int_0^k \right) - a$$

$$z = -a + ib + ib \frac{\int_0^k}{k}$$

Obviously, the last term of the last equation is likewise real, \int_k^1 contains two roots with negative radicands and it follows, of necessity, that

$$ib \frac{\int_0^k}{k} = +a$$

in order to satisfy conditions at point D where $t \rightarrow 1$. Thus we obtain for the (real) aspect ratio of the rectangular quadrant in terms of the abbreviated integrals for the imaginary terms

$$\frac{a}{b} = \frac{\int_0^k}{k} \quad [33]$$

Hence, for the segment CD in the z -plane the following equation applies:

$$z = a + ib \left(1 + \frac{\int_0^k}{k} \right)$$

The segment DE in the t -plane is finally traversed for $1 < t < \infty$. In the integrand there now appear three imaginary roots and thus we obtain

$$z = \frac{ib}{k} \int_0^t - a = \frac{ib}{k} \left(\int_0^k + \int_k^1 + \int_1^t \right) - a$$

and with the value just obtained for $t = 1$ we have

$$z = ib \left(1 + \int_0^t \frac{1}{k} \right)$$

where z is purely imaginary and goes from $+ib$ to $+i\infty$.

Thus we have proved that the function [30] actually transforms the real u -axis of the t -plane into the polygon $ABCDE$ of the z -plane. Likewise it can be proved in an analogous manner by means of [30], that the interior of the polygon is obtained from the lower half of the t -plane. For the sake of completeness, let us further point out certain points of the z -plane at which the representation is not conformal. At the points B and D the integrand has singularities (∞) and the transformation function no longer is analytic and at the point C the derivative $\frac{dz}{dt} = 0$; it follows from this that at the points B , C , and D , the conformity of the representation is no longer retained. Hence, one excludes these points in the t -plane by by-passing them with small circles.

We can now proceed to utilize these relations just obtained to determine the hydrodynamic mass of polygons. We shall begin with the determination of the complex potential function for the absolute flow about a rectangular cross section:

At the boundary of any arbitrary cross section moving in a straight line (see Figure 16), the normal component of the fluid velocity $\frac{\partial \phi}{\partial r} = \frac{\partial \psi}{\partial s}$ must coincide with the velocity of the boundary itself along the normal. The velocity of the boundary in the direction of the normal is

$$U \cos \alpha = U \frac{dy}{ds}$$

from which we obtain

$$\frac{\partial \psi}{\partial s} = U \frac{dy}{ds}$$

and by integration along the boundary it follows that

$$\psi = U y + \text{const} \quad [34]$$

a relation which has already been used previously in Equation [23]. At infinity, moreover, the velocity, and also ϕ and ψ , must be equal to zero; with this and by [34], the conditions on the entire boundary of the field of flow in the $z = x + iy$ -plane are given.

Because of the double symmetry of the rectangular

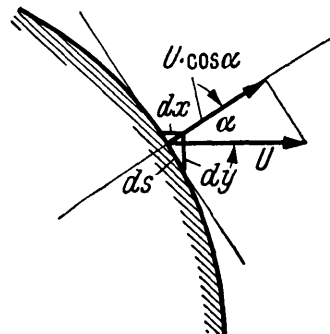
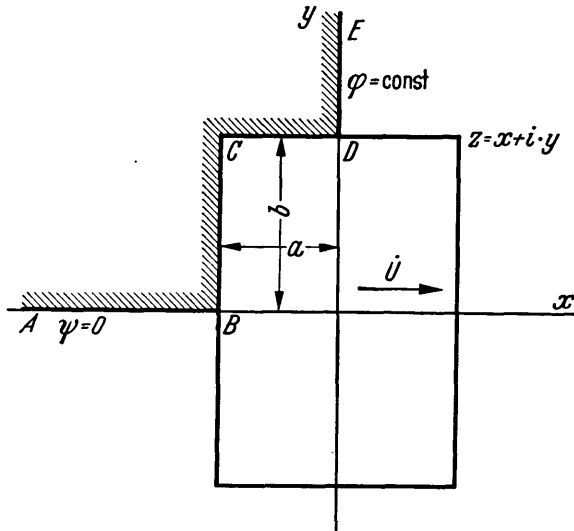


Figure 16 - Derivation of the Boundary Condition in the Case of Translation

Figure 17 - z -Plane

cross section now being considered (see Figure 17), it suffices to investigate the conditions in only one quadrant of the field. The boundary conditions for such a quadrant are found as follows: For the motion in the $+x$ -direction AB must be a streamline for reasons of symmetry; hence, the following condition must apply on AB

$$\frac{\partial \psi}{\partial x} = \frac{\partial \phi}{\partial y} = 0$$

or

$$\psi = \text{const}$$

and the constant may be set equal to zero

without restricting the generality. On DE , the velocity of the absolute flow must be equal to zero. Therefore, DE is a potential line, and the tangential derivative $\frac{\partial \phi}{\partial y}$ must vanish along it.

In order to obtain a region in which we can easily find the analytical function which satisfies the boundary conditions, the region $ABCDE$ in the z -plane is mapped into a half-strip in the ζ -plane. This is accomplished by mapping the z -plane and hence also the $\zeta = \xi + i\eta$ -plane, in which the region is represented by a half-strip, into the t -plane. The first transformation is made by means of Equation [30]; hence, the following condition applies on the boundary BC of the quadrant in the z -plane

$$z = iy = ib \int_0^t \frac{1}{k} dt - a$$

for $0 < t < k$; thus the boundary condition [34] is

$$\psi = Ub \int_0^t \frac{1}{k} dt + \text{const} \quad [35]$$

and in an analogous manner we obtain for the boundary segment CD , $k < t < 1$

$$\psi = Ub + \text{const} \quad [36]$$

As the second transformation we put

$$\zeta = h \int_0^t (0-t)^{-\frac{1}{2}} (1-t)^{-\frac{1}{2}} dt + h' \quad [37]$$

from which we get by integration (see Hütte, 26th edition, page 91)

$$\zeta = h \operatorname{arc} \cosh (1 - 2t) + h'$$

or written in a different form

$$1 - 2t = \cosh \left[\frac{\zeta}{h} - \frac{h'}{h} \right] \quad [38]$$

We shall now dispose of h and h' in such a manner that we obtain a half-strip open toward the right whose distance from the ξ -axis is $\pi/2$ and whose width is $\pi/2$ (see Figure 18). It will be immediately apparent why we choose a half-strip of exactly this width and position. If we set $h = 1/2$ and $h' = i \frac{\pi}{2}$, we obtain

$$1 - 2t = \cosh (2\zeta - i\pi) \quad [39]$$

This equation is obviously satisfied for $\zeta = i \frac{\pi}{2} (\cosh i\eta = \cos \eta)$; therefore, point B ($t = 0$) maps into $\zeta = 0 + i \frac{\pi}{2}$. For $t = 1$ it follows that $-1 = \cosh (2\zeta - i\pi)$; which is satisfied for $\zeta = 0 + i\pi$. For the segments AB ($t < 0$) and DE ($t > 1$), the integrand of [37] becomes real and in the ζ -plane we obtain straight lines that are parallel to the ξ -axis (see Figure 18).

The significance of this last representation lies in the fact that in the half-strip we easily succeed in finding the analytic function which satisfies the boundary conditions. In the z -plane Equations [35] and [36] must be satisfied on BCD ; the segment BCD is now transformed into the segment of ζ -plane designated by the same letters in such a way that the potential on the boundary must remain invariant under the transformation. Hence, if we develop the expressions [35] and [36] on BCD into a cosine series, viz.,

$$\psi = Ub \int_0^t \frac{o}{k} + \text{const} = Ub (\alpha_0 + \alpha_1 \cos \eta + \alpha_2 \cos 2\eta + \dots + \alpha_n \cos n\eta) \quad [40]$$

where for $0 < t < k$ $\int_0^t = \int_0^t$ and for $k < t < 1$ $\int_0^t \equiv \int_0^k$, or if the constants on each side of the equation are set equal to zero, we obtain from [40] the expression in η :

$$\psi = Ub \int_k^o \frac{o}{k} = Ub (\alpha_1 \cos \eta + \alpha_2 \cos 2\eta + \dots + \alpha_n \cos n\eta) \quad [41]$$

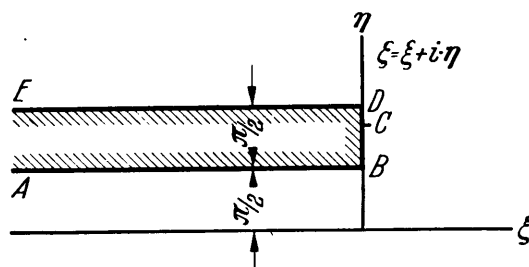


Figure 18 - ζ -Plane

which satisfies the boundary condition on BCD in the ζ -plane. For the entire half-strip $ABCDE$ it follows that

$$\psi = Ub (\alpha_1 e^{-\xi} \cos \eta + \dots + \alpha_n e^{-n\xi} \cos n \eta) \quad [42]$$

$$\varphi = \int \frac{\partial \psi}{\partial \eta} d \xi = Ub (\alpha_1 e^{-\xi} \sin \eta + \dots + \alpha_n e^{-n\xi} \sin n \eta) \quad [43]$$

since these functions fulfill all the necessary boundary conditions, i.e., they vanish for $\xi \rightarrow \infty$, ψ assumes the desired value [40] on BCD at $\xi = 0$ and the value $\psi = 0^*$ on AB , where $\eta = \frac{\pi}{2}$, while ϕ contains a vanishing tangential derivative $\frac{\partial \phi}{\partial \xi}$ on DE where $\eta = \pi$. The function $\phi + i\psi$, furthermore, is analytic which is already apparent from its formation by means of the Cauchy-Riemann differential equations. Thus, it represents the only analytic function which satisfies the boundary conditions and consequently it must be the complex potential function for the half-strip.

Since the kinetic energy is also invariant under the transformations, the kinetic energy of this field of flow in the ζ -plane also represents the kinetic energy in the initial field in the z -plane and thus represents the solution of the problem.

In carrying out the actual calculation, we proceed as follows: First we develop the differential quotient $\frac{dz}{dt}$, abbreviated by c , from Equation [30]

$$\frac{(k-t)^{\frac{1}{2}}}{(-t)^{\frac{1}{2}} (1-t)^{\frac{1}{2}}} \quad [44]$$

where we assume for k any arbitrary value between 0 and 1. The function which is represented graphically by the curves in Figure 19 is then subjected to a continuous numerical integration in which the improper integrals which occur in the vicinity of the zeros of the denominator are to be evaluated by substituting an equivalent analytic expression. On integration we obtain the Schwarz-Christoffel function, abbreviated by c , $z = \int_0^t$, i.e., Equation [30], in the form of a table from which we can find the aspect ratio of the rectangle, determined by k , with the aid of Equation [33], viz., $\frac{a}{b} = \int_k^1 / \int_0^k$. We then trace the integral curve \int_0^t / \int_0^k , which, in each case, reaches its peak value 1 at the point $t = k$ and then, because $\int_0^t = \int_0^k$ for $k < t < 1$, retains this ordinate. For the abscissa Equation [38] reduces to

$$1 - 2t = \cosh (2 \xi - i \pi)$$

For the imaginary axis, this relation may be written more simply as

$$1 - 2t = \cos (2\eta - \pi)$$

*Since the function $\psi = f(\eta)$ must be antisymmetric about $\pi/2$ according to its symmetry characteristics shown in Figure 17, the terms in the series with even index must vanish as these terms are symmetrical with respect to $\pi/2$.

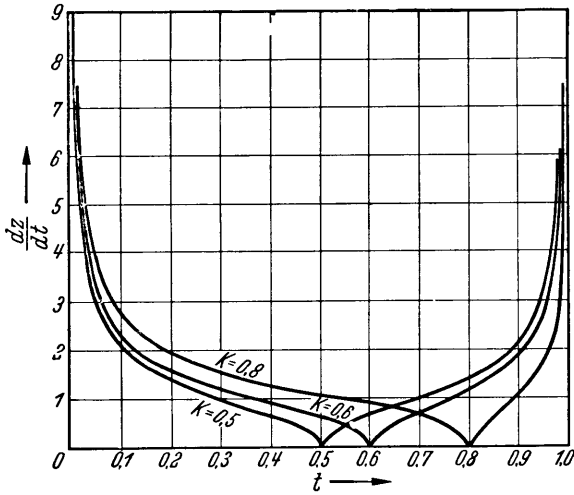


Figure 19 - Development of $\frac{dz}{dt}$ Equation [44]

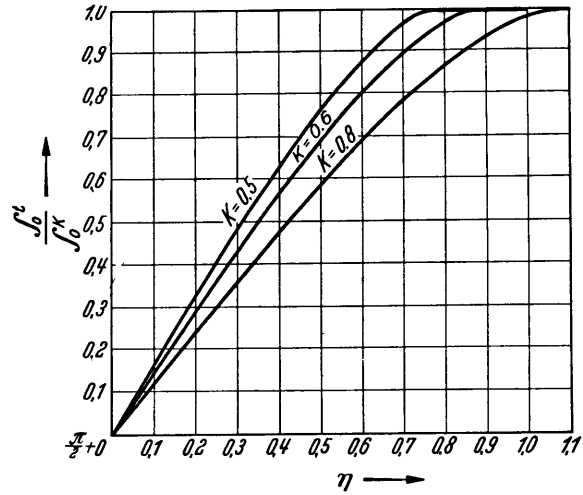


Figure 20 - $\int_0^t \frac{dz}{dt^k}$ As a Function of η

or

$$t = \frac{1}{2} (1 + \cos 2\eta) = \cos^2 \eta \quad [45]$$

where, with the aid of the last expression, the negative root for $\cos \eta$ is to be taken. The

function plotted in Figure 20 $\int_0^t \frac{dz}{dt^k} = f(\eta)$ is then approximated by means of Runge's method*
by means of a cosine series

$$a_1 \cos \eta + a_2 \cos 2\eta + \dots + a_n \cos n\eta = \sum_{n=1}^{n=\infty} a_n \cos n\eta$$

On the boundary BD , we thus have

$$\psi = Ub \sum_{n=1}^{n=\infty} a_n \sin n\eta$$

and

$$\varphi = Ub \sum_1^{\infty} a_n \sin n\eta$$

For the half-strip the kinetic energy then amounts to

*Runge's method for representing a numerically expressed function by means of a Fourier series.¹⁷

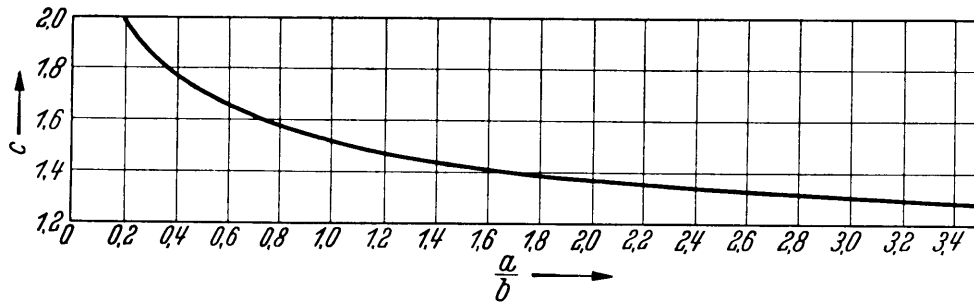


Figure 21 - Inertia Coefficients for the Rectangle
For part of the data Lewis's values were used.

$$2 T = -\rho \int_{\frac{\pi}{2}}^{\pi} \varphi \frac{\partial \varphi}{\partial \xi} d \eta$$

$$2 T = \rho U^2 b^2 \int_{\frac{\pi}{2}}^{\pi} (\sum a_n \sin n \eta)^2 d \eta$$

$$2 T = \frac{\pi}{4} \rho U^2 b^2 (a_1^2 + 2a_2^2 + \dots + n a_n^2)$$

Then for the entire rectangle we need four times this value or

$$T = \frac{\pi}{2} \rho U^2 b^2 (a_1^2 + 2a_2^2 + \dots + n a_n^2) \quad [46]$$

and because $T = \frac{m''}{2} \cdot U^2$, we have for the hydrodynamic mass of the rectangle in translation

$$m'' = \pi \rho b^2 (a_1^2 + 2a_2^2 + \dots + n a_n^2) \quad [47]$$

On the basis of the method described here, the calculation was carried out, for various forms including the square ($k = 0.5$); after developing the cosine series up to the 18th term, m'' was found to equal $1.512 \pi \rho b^2$. The inertia coefficient C is therefore 1.512. Lewis, by another method, found $C = 1.5131$. In Figure 21, the inertia coefficients for the rectangle are plotted as a function of the aspect ratio (see also Figure 10). The values determined experimentally by Koch for rectangles by means of the electrical analogue—for example, $C = 1.67$ for the square—likewise show but a moderate deviation due to the fact that in the experiment it is possible to satisfy the boundary conditions only approximately; for many practical purposes, however, this deviation is acceptable.

In general, the Schwarz-Christoffel function yields hyperelliptic integrals which do not permit an evaluation in closed form. In the case of simple cross sections, such as rectangles, it is possible to reduce the transformation integral to tabulated elliptic integrals. Since, in

the present paper, however, we are not generally dealing with such simple cross sections, we refrained in all cases from the reduction to Legendre's standard forms in order to maintain a greater uniformity in our treatment.

For the limiting case of the flat plate of the width $2b$ for which we have to put $k = 1$, we obtain an elementary integral, hence, this case will also be discussed. The stream-function on the surface of the plate moving normal to its plane must be as follows (see Figure 22):

$$\psi = Ub \int_0^t \frac{1}{1-t} dt \text{ for } 0 < t < 1$$

with the integrand

$$\frac{(1-t)^{\frac{1}{2}}}{(-t)^{\frac{1}{2}} (1-t)^{\frac{1}{2}}} = \frac{1}{\sqrt{-t}}$$

and the integrals

$$\int_0^t \frac{1}{\sqrt{-t}} dt = 2i \sqrt{t}$$

$$\int_0^1 \frac{1}{\sqrt{-t}} dt = 2i$$

Therefore, the following equation holds:

$$\psi = Ub \sqrt{t}$$

For the imaginary axis, the representation of the t -plane in the ζ -plane is again made by means of the function $t = \cos^2 \eta$; the following, therefore, applies in the ζ -plane on the boundary of the plate

$$\psi = Ub \cos \eta$$

and throughout the entire field

$$\psi = Ub e^{-\xi} \cos \eta$$

$$\varphi = Ub e^{-\xi} \sin \eta$$

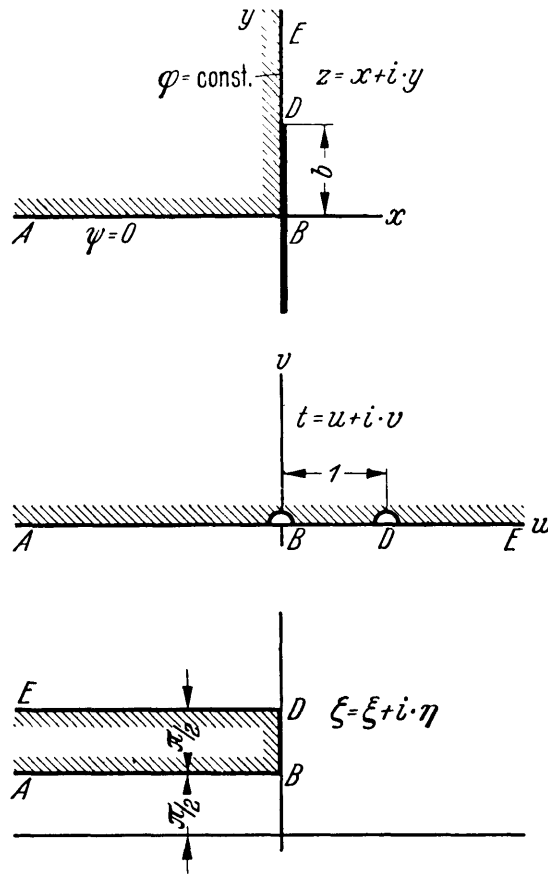


Figure 22 - Representation for Flow About the Plate

The energy integral vanishes everywhere except for the boundary segment BD and here, i.e., on the quadrant in the z -plane, it yields

$$2 T = \frac{\pi}{4} \rho U^2 b^2$$

and for hydrodynamic mass of the plate of the width $2b$ we obtain

$$m'' = \pi \rho b^2$$

and for the inertia coefficient

$$C = 1$$

which is the familiar solution for the plate as the limiting case of the ellipse (see Section 9).

12. THE HYDRODYNAMIC MASS FOR A RECTANGULAR CROSS SECTION PROVIDED WITH BILGE KEELS

In the case of the rectangle with bilge keels moving in translation in the $+x$ -direction (see Figure 23), it is again sufficient, because of the double symmetry, to limit the calculation to one quadrant (see Figure 24). The problem is to find an analytical function which satisfies the boundary condition $\psi = Uy$ on $BCDEF$, the condition $\psi = 0$ on AB and the condition $\frac{\partial \phi}{\partial y} = 0$ on FG . In order to determine the function which satisfies these conditions, we again map the polygon in the z -plane (see Figure 24) into a suitable half-strip in the ζ -plane (Figure 26) which can easily be accomplished by mapping the upper half-plane of the auxiliary t -plane (Figure 25) into each of these regions.

The transformation of t into z is as follows:

$$z = c \int_0^t (0-t)^{-\frac{1}{2}} (k-t)^{-\frac{1}{4}} (l-t)^{+1} (m-t)^{-\frac{1}{4}} (1-t)^{-\frac{1}{2}} dt + c' \quad [48]$$

for which, if we take the vertex at infinity into consideration, we obtain the sum of the exponents $\sum \mu_i = 2\pi$, as required. Since for $t = 0$, z should again equal $-a$, we obtain for the constants c and c'

$$c' = -a$$

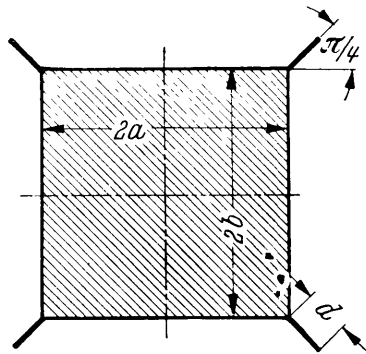


Figure 23 - Rectangle with Bilge Keels

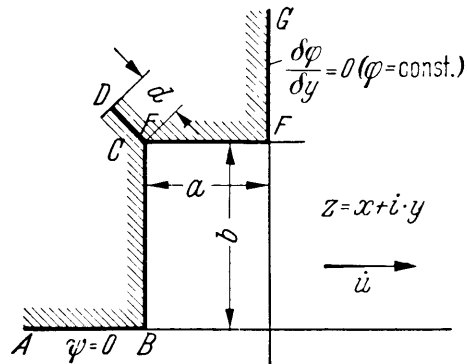


Figure 24 - Quadrant of the Rectangle with Bilge Keels

and furthermore since for $t = k$, z should be equal to $-a + ib$, we have

$$c = \frac{ib}{\int_0^k}$$

As c and c' are fixed and there are no other constants available, we have for $t = 1$

$$z = ib \frac{\int_0^1}{\int_0^k} - a = 0 + ib$$

We divide this expression up into its separate integrals, wherein each integral is evaluated over that segment in the z -plane designated by the arrow, by integrating from the lower to upper limit

$$z = \frac{ib}{\int_0^k} \left[\int_0^k + \int_k^l - \int_l^m + \int_m^1 \right] - a \tag{49}$$

Hence, the following must hold:

$$\int_k^l = \int_l^m,$$

$$d = ib \frac{\int_k^l}{\int_0^k}$$

from which, by abbreviating the imaginary quantity for the ratio of the height of the bilge keel to the half-length, we obtain

$$\frac{d}{b} = \frac{\int_k^l}{\int_0^k}$$

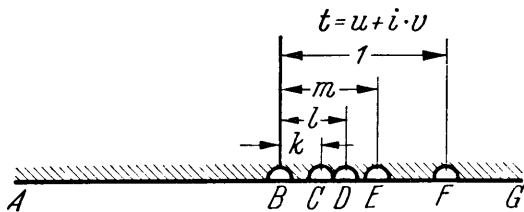


Figure 25 - t -Plane

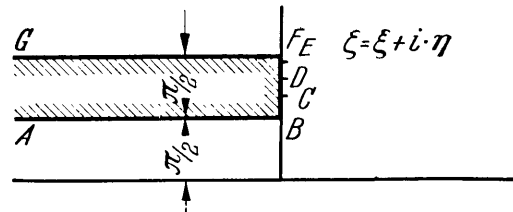


Figure 26 - ζ -Plane

and for the ratio of the sides themselves

$$\frac{a}{b} = \frac{\int_0^1 m}{\int_0^1 k}$$

The ratio d/b , hence the height of the bilge keel, as well as a/b , the aspect ratio of the rectangular cross section, can be determined from the values k and l which are selected arbitrarily but in the proper sequence between 0 and 1; however, once k and l are selected, m is determined so that $\int_k^l = \int_l^m$ is satisfied; otherwise we would not obtain the desired form in which the points C and F are supposed to have the same coordinates. If, in particular, the basic rectangle used is a square, then the following equation must apply: $\int_m^1 = \int_0^k$.

The mapping of the t -plane into the half-strip of the ζ -plane is accomplished, as described above (see Section 11), by relation [39]; thus for the boundary segment BF which is purely imaginary in the ζ -plane, we obtain specifically Equation [45] once again. If we now make use of the relations for y from Equation [49] for $z = x + iy$ and if we introduce these into the boundary condition $\psi = Uy$, we obtain ψ as $f(t)$ on $BCDEF$. By means of Equation [45] relating t as a function of η , we obtain $\psi = f(\eta)$. Finally, we again develop ψ on the boundary $BCDEF$ into a cosine series in η

$$\psi = Ub \sum_1^{\infty} a_n \cos n \eta$$

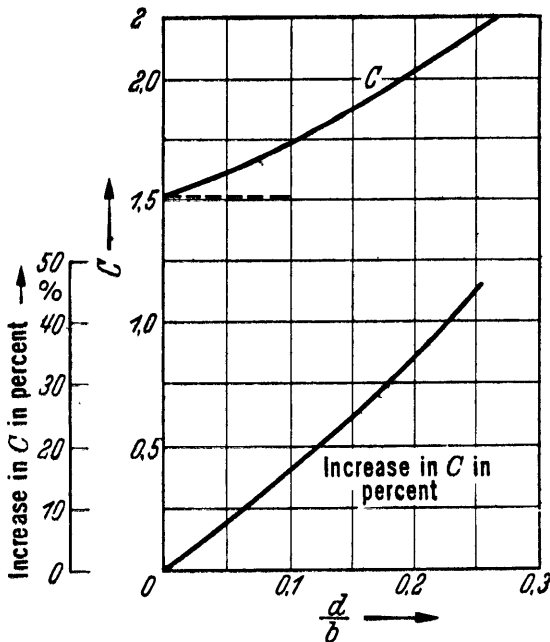


Figure 27 - Inertia Coefficient C and Its Percentage Increase for a Square Cross Section with Bilge Keels of Various Heights

and obtain ψ , ϕ , and $\frac{\partial \phi}{\partial \xi}$ on the boundary and with these quantities, the kinetic energy of the field. The calculation was confined to the case of the square ($a = b$) as the basic cross section and it was carried out for three bilge keel heights defined by the ratio d/b . We obtained the following table (see Figure 27),

TABLE 1

d/b	m''	C	Increase in C in percent
0	$1.512 \pi \rho b^2$	1.512	0
0.0494	$1.61 \pi \rho b^2$	1.61	6.74
0.123	$1.80 \pi \rho b^2$	1.80	19.05
0.2278	$2.11 \pi \rho b^2$	2.11	39.5

where the length $2b$ of side of the square cross section was chosen in all cases as the reference width for determining C ; hence the hydrodynamic mass is given by $m'' = C \pi \rho b^2$. The percent increase in the inertia coefficient C for the square with the bilge keel compared with the value without the keel was calculated by the expression

$$\text{Percentage increase in } C = \frac{C_{\square \text{ with keel}} - C_{\square}}{C_{\square}} \cdot 100$$

13. DISTRIBUTION OF THE ACCELERATION PRESSURES OVER SOME OF THE CROSS-SECTIONAL FORMS INVESTIGATED

If we designate the acceleration pressure by p_B , then the equation (see Section 8) defining the hydrodynamic mass for motion in the x -direction is

$$\int_s p_B \cos \alpha \, ds = m'' \dot{U} \quad [50]$$

with $\cos \alpha$ as the direction cosine of the outward drawn normal to the surface element ds . Conversely, if we find a relation for the hydrodynamic mass by integration over the cross-sectional boundary, we can determine the acceleration pressures. Accordingly, for the rectangle moving in the x -direction, we have

$$p_B = \frac{dm''}{dy} \dot{U} \quad [51]$$

since the components of the compressive force are zero on the sides parallel to the x -axis. In the ζ -plane, the pressure on the segment which transforms into the boundary of the body is

$$p_B = \frac{dm''}{d\eta} \dot{U} = \rho \varphi \frac{\partial \varphi}{\partial \xi} \frac{\dot{U}}{U^2}$$

Using the expression for ϕ , Equation [43], it follows that

$$\frac{dm''}{d\eta} = \rho b^2 \sum_{n=1}^{n=\infty} \sum_{m=1}^{m=\infty} a \sin n \eta \cdot a_m m \sin m \eta$$

Also on the η -axis of the ζ -plane, relation [45] holds

$$t = \frac{1}{2} (1 + \cos 2\eta)$$

whence with

$$d\eta = - \frac{dt}{\sin 2\eta}$$

we obtain

$$\frac{dm''}{dt} = -\varrho b^2 \frac{1}{\sin 2\eta} \sum_{n,m=1}^{n,m=\infty} a_n \sin n\eta a_m m \sin m\eta \quad [52]$$

In like manner, from the transformation of the t -plane into the z -plane

$$dt = \frac{\int_0^k}{b} \cdot \frac{(-t)^{\frac{1}{2}} (1-t)^{\frac{1}{2}}}{(k-t)^{\frac{1}{2}}} dy$$

we finally arrive at the relation

$$\frac{p_B}{\varrho b \dot{U}} = \frac{1}{\varrho b} \frac{dm''}{dy} = \frac{\int_0^k}{\sin 2\eta} \cdot \frac{(-t)^{\frac{1}{2}} (1-t)^{\frac{1}{2}}}{(k-t)^{\frac{1}{2}}} \sum_{n,m=1}^{n,m=\infty} a_n \sin n\eta a_m m \sin m\eta \quad [53]$$

from which the pressure distribution can be determined point-by-point.

In actual practice, we proceed as follows:

1. t is given and the corresponding value of η is also known by means of [45].

2. $y = b \frac{\int_0^t}{k}$ gives us, for $0 < t < k$, the corresponding value of y and for $k < t < 1$, $y = b$.

3. The series $\sum_{n,m=1}^{n,m=\infty}$ is the product of the two series

$$\sum_{n=1}^{n=\infty} a_n \sin n\eta = a_1 \sin \eta + a_3 \sin 3\eta + \dots + a_{2n+1} \sin (2n+1)\eta$$

and

$$\sum_{m=1}^{m=\infty} a_m m \sin m\eta = a_1 \sin \eta + 3a_3 \sin 3\eta + \dots + (2m+1) a_{2m+1} \sin (2m+1)\eta$$

if we confine the calculation to the square for which the even terms of the series vanish as y is antisymmetric with respect to $\pi/2$, see Figure 20. For the product of these series, we have considered the terms up to $n, m = 11$; we then obtain

$$\begin{aligned} \sum_{n,m=1}^{n,m=11} &= a_1^2 \sin^2 \eta + 3a_3^2 \sin^2 3\eta + \dots + 11a_{11}^2 \sin^2 11\eta + 4a_1 a_3 \sin \eta \sin 3\eta \\ &+ \dots + 20a_9 a_{11} \sin 9\eta \sin 11\eta \end{aligned}$$

4. For each group of values t, η, y we then calculate the differential quotient $\frac{\partial \eta''}{\partial y}$ and the dimensionless expression [53] $\frac{p_B}{\rho b U}$ for the acceleration pressures. By plotting these values against y we obtain the desired pressure distribution (see Figure 28).

In a wholly analogous manner, we determine the acceleration pressures for the square cross section with bilge keels (see Figure 29). In this case, too, there exists symmetry with respect to a diagonal drawn through zero at an angle of 45 degrees; hence the series development remains correct, but the coefficients a_n and a_m are of course different. By differentiating the transformation function [49] with respect to t and by introducing the differential quotients obtained for the individual boundary segments into [52], we obtain, after several additional transformations of the type already carried out in the case of the square, the relations for the acceleration pressures on the individual boundary segments. The numerical evaluation yields the pressure distribution, plotted in Figure 30, for keel heights $\frac{d}{b} = 0.0494$ and $\frac{d}{b} = 0.2278$. By this method, we obtain infinite pressures at the sharp corners of rectilinear cross sections. Since on real bodies the radii of curvature are always different from zero, we would obtain finite pressures even if we assume an ideal fluid.

The pressure distribution on transverse sections with considerable curvature is likewise of interest. (See Sections 8 and 9.) For the translational motion in the x -direction of a cross section with semi-axes $X = Y = 1 + b$, we obtain for the energy of flow field

$$2 T = m'' U^2 = \rho U^2 \int_0^{2\pi} (\cos \Theta - b \cos 3 \Theta) (\cos \Theta - 3 b \cos 3 \Theta) d \Theta$$

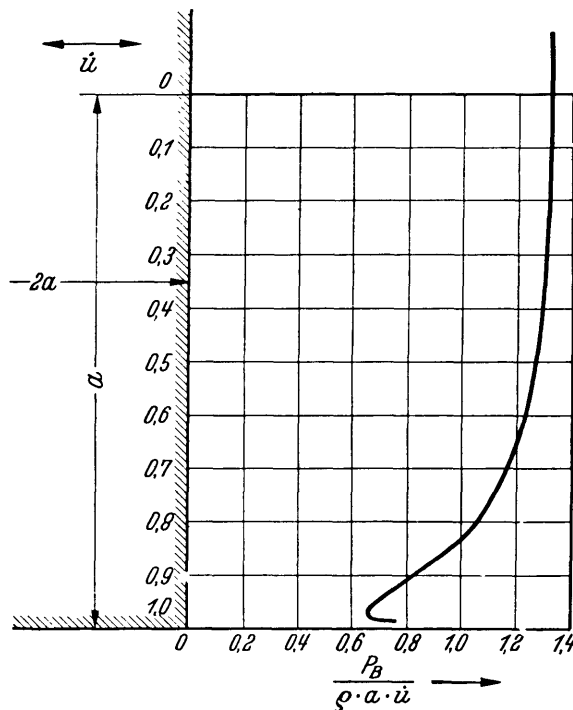


Figure 28 - Distribution of the Acceleration Pressure for the Case of the Square in Translation

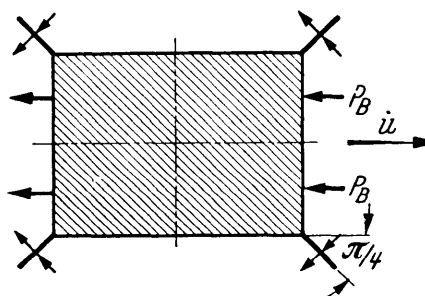


Figure 29 - Acceleration Pressures for the Case of the Rectangle with Bilge Keels

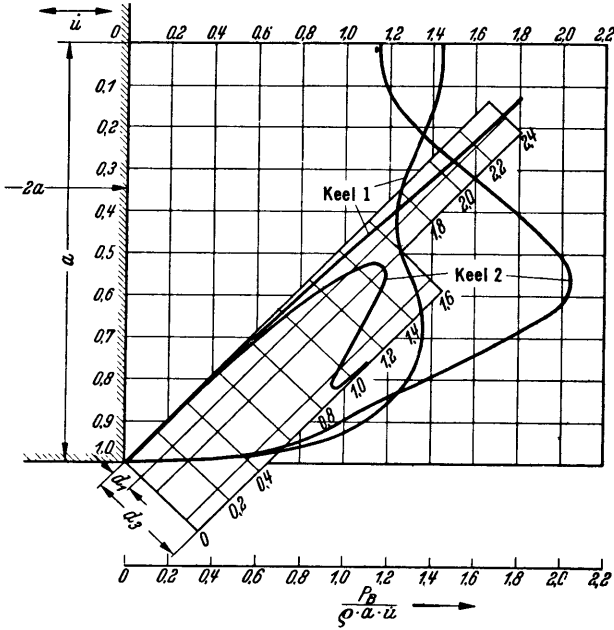


Figure 30 - Acceleration Pressures for the Case of the Square with Bilge Keels
Keel 1: $d/b = 0.049$; Keel 2: $d/b = 0.228$

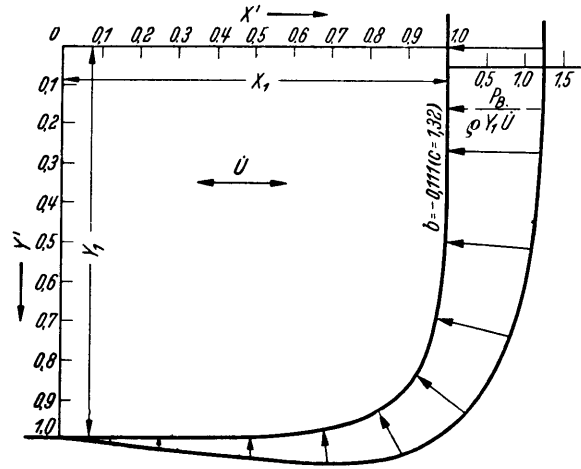


Figure 31 - Distribution of the Acceleration Pressures for the Case of a Transverse Section Profile

The acceleration pressure, Equation [50], amounts to :

$$p_B = \frac{dm''}{dY} \frac{1}{\cos \alpha} \dot{U}$$

where α denotes the direction which the normal to the surface element makes with the horizontal. We find, moreover, that by Equation [24]

$$Y = \sin \Theta - b \sin 3 \Theta$$

thus

$$\frac{dm''}{dY} = \frac{dm''}{d\Theta} \frac{d\Theta}{dY} = \rho (\cos \Theta - b \cos 3 \Theta)$$

and thereby

$$p_B = \rho (\cos \Theta - b \cos 3 \Theta) \frac{1}{\cos \alpha} \dot{U}$$

For the purpose of plotting, we form the dimensionless expression

$$\frac{p_B}{\rho Y_1 \dot{U}} = (\cos \Theta - b \cos 3 \Theta) \frac{1}{Y} \frac{1}{\cos \alpha}$$

or if, for the sake of a better comparison with the above-mentioned cross sections, the semi-axes are put equal to 1:

$$\frac{p_B}{\rho Y_1 \dot{U}} = (\cos \Theta - b \cos 3 \Theta) \frac{1}{1+b} \frac{1}{\cos \alpha} \tag{54}$$

The normal pressures $\frac{p_B}{\rho Y_1 U}$ calculated in this manner are plotted in Figure 31 for the form $b = -0.111$.

14. COMPARISON OF RESULTS WITH EXPERIMENTS

Experiments with rectangular cross sections executing translational oscillations have been carried out by Nicholls,¹⁸ Moullin,¹⁹ and Holstein.¹⁴

Nicholls fastened a block of wood to a steel plate to form a prism of cross section 2×1.562 inches and set it into vibration normal to the water surface. As will be seen later on, a body oscillating normal to the water surface is, under certain conditions, mathematically equivalent to a double body formed by the body and its mirror image in the water surface and oscillating in an infinite medium. Hence, the inertia coefficient C , for the submerged part of the body, has the same value it would have in an infinite medium. Nicholls measured the frequencies of the beam supported at the nodal points for the free-free oscillations both in air and in water. Later on Lewis explained the difference in frequencies as due to the hydrodynamic mass of the water which increases the effective mass taking part in the oscillation. Lewis determined the size and the approximate distribution of the hydrodynamic mass by means of the coefficients of inertia C (see Sections 4 and 9) and the coefficient of reduction R (see Section 6).

Moullin and Browne likewise conducted oscillation tests with a beam of rectangular section on the surface. A comparison shows that their results are in good agreement with the values calculated by Lewis, the measured values always lying between 90 and 100 percent of the calculated ones. As long as the length was greater than four times the width of the beam, the assumption of two-dimensional flow proved to be a satisfactory approximation.

A further means of verifying analytical results is provided by the experiments of Holstein already referred to above (see Section 7). On the basis of extensive tests with a rigid parallelepiped oscillating normal to the water surface, Holstein obtained values for the hydrodynamic mass which are plotted in Figure 32 as inertia coefficients C against the depth of immersion b in a manner suitable for drawing a comparison. Instead of a single-valued function the values fall within a strip because of the dependence of the hydrodynamic mass on frequency which Holstein established conclusively in his experiments for oscillations on a surface. According to the data of Holstein, the maximum error possible amounts to $\Delta C = \pm 0.175$; the theoretical curve likewise plotted in Figure 32 would fall entirely within the strip if its width were increased by this limit of error. Moreover, we have previously pointed out the moderate rounding off of the corners on the body tested by Holstein. A calculation based upon the resultant deviation from a sharp cornered profile results in a slight diminution of the coefficient C . For high-frequency oscillations the dependence on frequency must be reduced to a minimum (as will be seen in Section 19 later on); this is verified by the fact that the upper limiting curve of the strip was obtained for the fastest oscillations; it should be noted in this connection that even for these oscillations the frequency amounted to

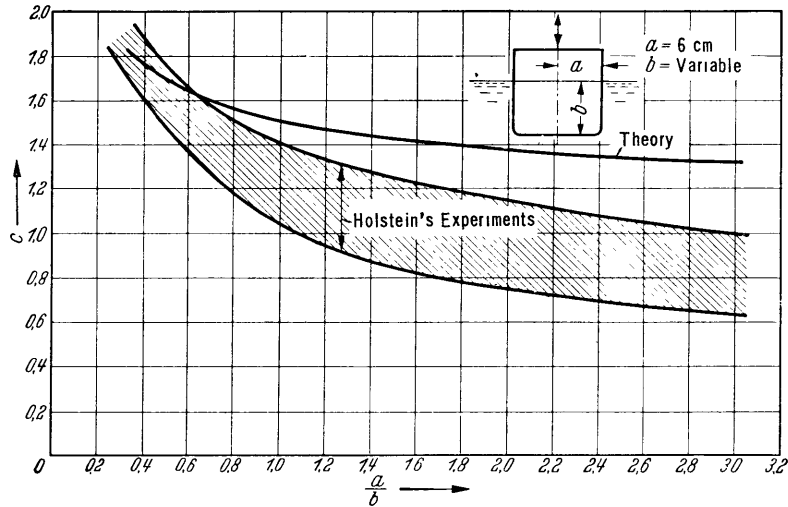


Figure 32 - Inertia Coefficients from Holstein's Experiments and from Theory

only about 2.5 hertz so that it lies approximately in the range of the frequencies observed for flexural vibrations of ship hulls. The condition proved experimentally by Holstein that at a greater depth of immersion, the hydrodynamic mass increases even though the lower surface of the parallelepiped acted upon by the water remains the same, is completely confirmed by a corresponding rise in the theoretically determined curve (see Figure 32) for smaller values of the aspect ratio a/b . The change in the field of flow caused by a greater depth of immersion of the parallelepiped, with the same lower surface normal to the direction of motion, results in a greater kinetic energy.

III. HYDRODYNAMIC MOMENTS OF INERTIA

15. HYDRODYNAMIC MOMENTS OF INERTIA ALREADY DETERMINED ANALYTICALLY

Thus far, hydrodynamic moments of inertia have been calculated only in individual cases. In addition to the elliptical section dealt with in the textbooks of hydrodynamics (see also Section 5 of this treatise), only Proudman's solutions for the square²⁰ and Weinblum's solutions for the regular octagon²² have come to the attention of the author.

Before we proceed to determine a number of additional moments of inertia, we shall introduce a coefficient D for rotation which corresponds to the inertia coefficient C for translation. Since the hydrodynamic moment of inertia for the circular cylinder, in the case of rotation about the axis, turns out to have the trivial value zero, the circular section is ruled out as a reference cross section. The case of a rotating plate will be used as a reference section. This case which is the limiting case of an ellipse is integrable in closed form. Accordingly, the inertia coefficient for rotation D will be defined as follows:

$$D = \frac{J''}{J''_{\text{plate}}} \quad [55]$$

where J'' denotes the hydrodynamic moment of inertia of the section considered and J''_{plate} the hydrodynamic moment of inertia of the plate whose width $2b$ refers to a given characteristic dimension of the section under consideration. For the denominator we obtain, by the relation already given in Section 5,

$$J''_{\text{plate}} = \frac{1}{8} \pi \rho b^4 \quad [56]$$

Hence, from now on, the hydrodynamic moment of inertia will generally be

$$J'' = D \cdot J''_{\text{plate}} = D \cdot \frac{\pi}{8} \rho b^4 \quad [57]$$

where the length b in the following discussion is fixed in such a manner that in any cross section considered it has exactly the length of the segment of the y -axis.

The coefficient D will first be used to evaluate the hydrodynamic moment of inertia of the ellipse as a function of its length-width ratio a/b . From the relations [17] and [57] we obtain for the inertia coefficient

$$D = \frac{(\sqrt{a^2 - b^2})^4}{b^4} = \left[\left(\frac{a}{b} \right)^2 - 1 \right]^2 \quad [58]$$

This function has been plotted in Figure 33.

The inertia coefficient for the square section investigated by Proudman can be obtained as a special case from the following more general investigation of the rectangular section.

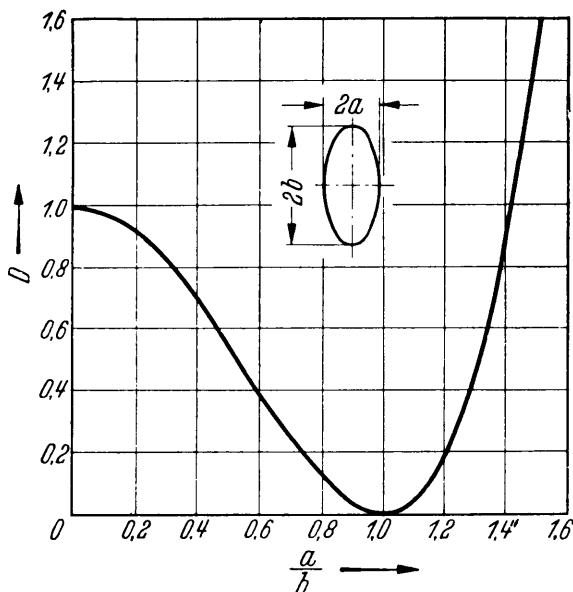


Figure 33 - Inertia Coefficient for Rotation of the Ellipse

For the octagon studied by Weinblum we obtain an inertia coefficient of $D = 0.44$. In determining the potential function, Proudman and Weinblum also made use of the method of direct solution of the boundary-value problem. Both authors selected regular polygons of very particular symmetry characteristics for their investigation with the result that the developments required for the solutions became exceedingly simple.

16. DETERMINATION OF THE HYDRODYNAMIC MOMENTS OF INERTIA OF RECTILINEAR SECTIONS

First of all, we shall again fix the boundary conditions which a body rotating about the origin must satisfy. The liquid is assumed to be at rest at infinity. The velocity of the liquid along the outward drawn normal $\left(\frac{\partial \phi}{\partial n} = \frac{\partial \psi}{\partial s}\right)$ must coincide with the velocity of the boundary itself. In the direction of the normal, the boundary has the velocity $\omega r \sin \alpha$ (see Figure 34); with $\sin \alpha = \frac{dr}{ds}$ we have

$$\omega r \frac{dr}{ds} = \frac{\partial \psi}{\partial s}$$

from which, by integration along the boundary of the body, we obtain

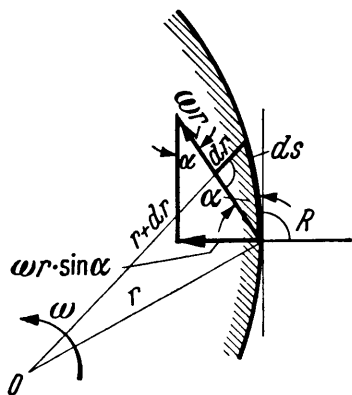


Figure 34 - Diagram for the Derivation of the Boundary Condition for Rotation

$$\psi = \omega \frac{r^2}{2} + \text{const} \quad [59]$$

An analytic function which satisfies this condition along the boundary of the section and which vanishes at infinity constitutes a solution of the boundary-value problem. There is only one such function and this function represents the complex potential for the flow.

If we consider once again the rectangular section (see Figure 13), we find that, because of the double symmetry, it is sufficient to study only one quadrant

(see Figure 35). AB and DE are the potential lines ($\phi = \text{constant}$); on AB and DE the equations $\frac{\partial \phi}{\partial x} = \frac{\partial \psi}{\partial y} = 0$ and $\frac{\partial \phi}{\partial y} = -\frac{\partial \psi}{\partial x} = 0$ must apply, respectively, and on the boundary of the rectangle BCD , the condition [59] or $\psi = \frac{1}{2} \omega \cdot (x^2 + y^2) + \text{const}$ must be satisfied. In order to find the potential function, we again map the polygon in the z -plane into a suitable half-strip in the ζ -plane by means of an auxiliary t -plane. The transformation of the t -plane (see Figure 36) into the z -plane is the same as the one already used in Section 11.

As a half-strip, we select the one drawn in Figure 37 which has the width π . The transformation of the t -plane into this half-strip is

$$\zeta = h \operatorname{arc} \cosh (1 - 2t) + h' \quad [60]$$

with $h = 1$ and $h' = 0$. As far as the details of the calculation are concerned, we again proceed in exactly the same manner as we did previously in connection with the computation of the hydrodynamic mass. We finally obtain for ψ on the boundary BD in the ζ -plane, the series

$$\psi = \frac{\omega}{2} b^2 \sum_{n=1}^{\infty} a_n \cos n \eta \quad [61]$$

and for the entire half-strip, the series

$$\psi = \frac{\omega}{2} b^2 \sum_1^{\infty} a_n e^{-n\xi} \cos n \eta \quad [62]$$

The kinetic energy for the entire rectangle is found to be

$$T = \frac{\pi}{2} \rho \omega^2 b^4 (a_1^2 + 2 a_2^2 + \dots + n a_n^2) \quad [63]$$

the hydrodynamic moment of inertia is

$$J'' = \frac{2 T}{\omega^2} = \pi \rho b^4 (a_1^2 + 2 a_2^2 + \dots + n a_n^2) \quad [34]$$

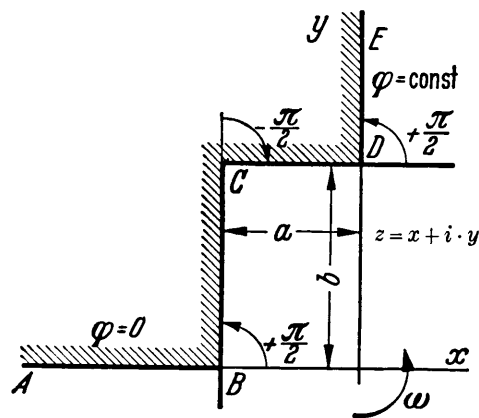


Figure 35 - z -Plane

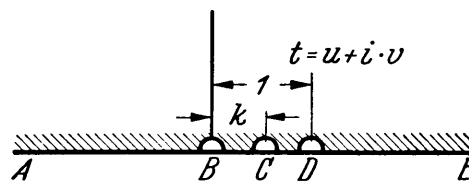


Figure 36 - t -Plane

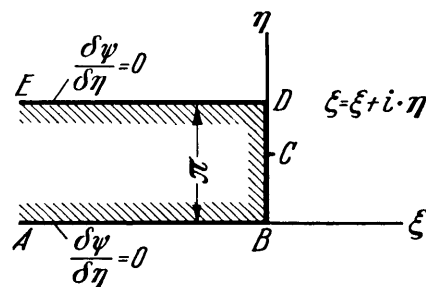


Figure 37 - ζ -Plane

and the inertia coefficient D is

$$D = \frac{\pi \rho l^4 \sum_1^{\infty} n a_n^2}{\frac{1}{8} \pi \rho l^4} = \frac{1}{8} \sum_1^{\infty} n \alpha_n^2 \quad [65]$$

For several aspect ratios a/b , J'' or D have been calculated numerically in essentially the same manner as that described in Section 11 for the hydrodynamic mass. The values found for J'' and D are given in Table 2. Figure 38 shows the coefficient D as a function of the aspect ratio.

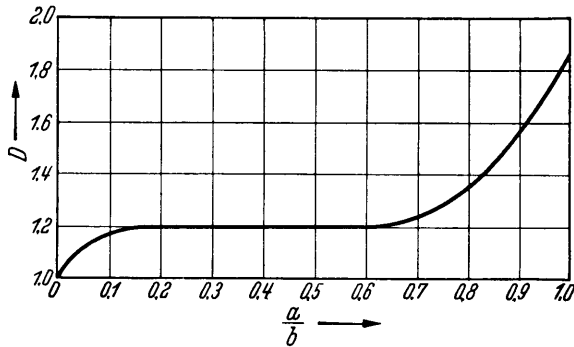


Figure 38 - Inertia Coefficient D for a Rectangle Rotating About Its Center

TABLE 2

k	a/b	J''	$D = \frac{J''}{\pi/8 \rho b^4}$
0.5	1	$0.234 \pi \rho b^4$	1.872
0.52	0.910	$0.198 \pi \rho b^4$	1.584
0.55	0.788	$0.166 \pi \rho b^4$	1.329
0.6	0.652	$0.152 \pi \rho b^4$	1.216
0.7	0.3985	$0.149 \pi \rho b^4$	1.192
0.8	0.2145	$0.150 \pi \rho b^4$	1.20
0.9	0.0782	$0.144 \pi \rho b^4$	1.152

Having determined D for aspect ratios in the range $0 \leq \frac{a}{b} \leq 1$, we know the inertia coefficients for all aspect ratios since we only have to take the reciprocal of the aspect ratio for values of a/b exceeding 1; in the case of rotation, it obviously does not matter in which direction the longest side of the rectangle runs. While D is nearly constant for $a/b < 0.6$, J'' becomes practically a parabola of the fourth degree when a/b exceeds ≈ 1.7 .

$$J'' \approx 0.15 \pi \rho b^4 \quad [66]$$

In this parabola, we naturally have to substitute for b half of the longest side of the rectangle.

In Figure 39, we indicate still another representation of the hydrodynamic components J'' to be added to the moments of inertia of the rigid body. If, for the prism of rectangular section and of the same density as the surrounding fluid, we designate the moment of inertia referred to the axis through the center of gravity by J_p , then the expression $(J''/J_p) \cdot 100$ indicates the percentage increase of the apparent moment of inertia as compared to the moment of inertia of the prism alone. This expression has been plotted against the aspect ratio in Figure 39.

These calculations were confined to the rectangular section. In an entirely analogous manner, the hydrodynamic moments of inertia of any arbitrary section can be determined as long as it has straight sides; all that is necessary is to set up a transformation which will

transform the Schwarz-Christoffel representation in the t -plane into the given polygon in the z -plane.

The flat plate is the limiting case of the rectangle as well as of the ellipse. If in the t -plane we put $k = 1$, we must obtain $a = 0$ and the aspect ratio a/b must also be equal to zero. While the integration in this case can be effected in an elementary fashion, we still want to verify the value

$$J'' = \frac{1}{8} \pi \cdot \rho \cdot b^4$$

which we know from the investigation of the ellipse is also obtained as the limiting case of the rectangle. For rotation about b , we must have on the boundary segment BD of the z -plane

$$\psi = \frac{\omega}{2} b^2 t$$

Over the entire half-strip in the ζ -plane we have

$$\zeta = \text{arc cosh} (1 - 2t)$$

$$1 - 2t = \cos \eta$$

$$t = \frac{1}{2} - \frac{\cos \eta}{2}$$

$$\psi = -\frac{\omega}{4} b^2 e^{-\xi} \cos \eta$$

With the resulting values of ϕ and $\frac{\partial \phi}{\partial \xi}$ the energy integral for the whole plate of width $2b$ gives

$$2 T = \frac{1}{8} \pi \rho \omega^2 b^4$$

and for the corresponding value of $J'' = \frac{1}{8} \pi \rho b^4$.

17. HYDRODYNAMIC MOMENTS OF INERTIA FOR A RECTANGULAR SECTION WITH BILGE KEELS

The rectangular section with bilge keels may also be regarded as a polygon. By means of Equation [49] already used above, the auxiliary t -plane is transformed into the z -plane. As ζ -plane we again select a half-strip of width π . The transformation of the t -plane into the

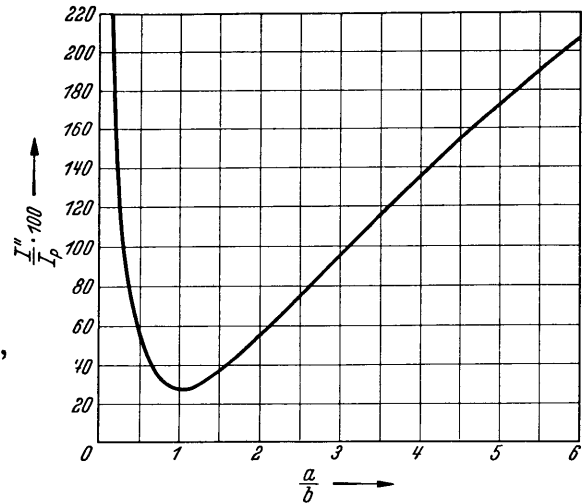


Figure 39 - Percentage Increase of the Apparent Moment of Inertia by the Surrounding Fluid

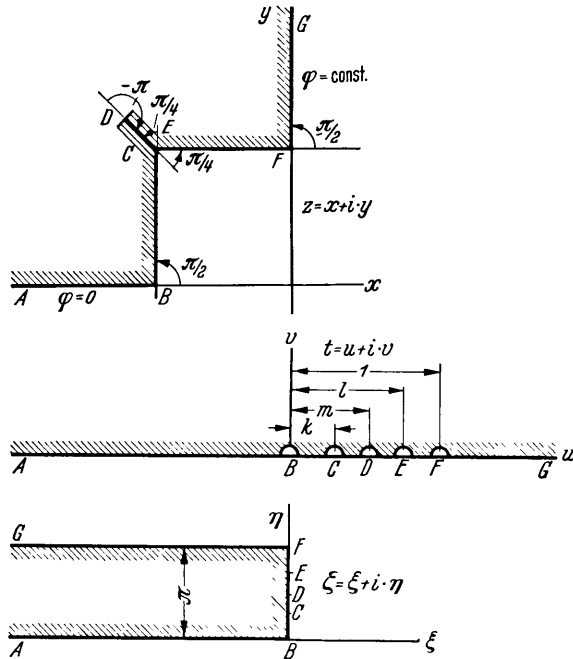


Figure 40 - Diagrams Used in Determining Potential of the Rotating Square with Bilge Keels

shows that the effect of the bilge keels on the increase of the hydrodynamic moment of inertia is far greater than it is on the increase of the hydrodynamic mass, a result which is to be expected on the basis of observation.

ζ -plane is given by the function [60] already used in the preceding section (see Figure 40).

The calculations which are fundamentally the same as those made for the simple rectangle were carried out for the square with bilge keels of the same heights as those previously treated in the case of translation (see Section 12). The calculation yielded the values given in Table 3 and Figure 41 in which b denotes half of the length of the square.

The percentage increase of D was calculated in comparison to the inertia coefficient for the square without keel, i.e.,

$$D = \frac{D_{\square \text{ with keels}} - D_{\square}}{D_{\square}} \cdot 100$$

A comparison of these values with those obtained for translation (see Section 12)

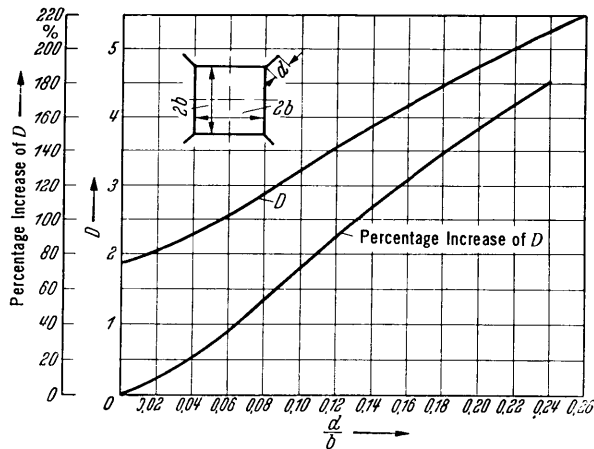


Figure 41 - Inertia Coefficient D and Percentage Increase for a Square Section with Bilge Keels of Various Heights

TABLE 3

d/b	J''	D	Percentage Increase of D
0	$0.234 \pi \rho b^4$	1.872	0
0.0494	$0.2995 \pi \rho b^4$	2.395	28
0.123	$0.450 \pi \rho b^4$	3.60	92.3
0.2278	$0.636 \pi \rho b^4$	5.09	172

18. COMPARISON OF RESULTS WITH EXPERIMENTS

Abell²¹ allowed a square prism standing upright to oscillate freely about its axis in a tank whose length was six times as long as the side of the square. The flow had been made two-dimensional by means of the tank bottom and a cover plate which left only a small space between the ends of the parallelepiped and the walls. Above the cover plate a plate was mounted on the axis for holding weights used to vary the period. Surface waves could not be generated since the tank was filled up to the cover plate.

From measurements of the natural period of this system in air and in water, Abell found that for the prism of square cross section the mass, which is conceived to be concentrated at a distance from the axis equal to the radius of gyration of the rigid square, must be increased by 28.5 percent of the mass of the displaced water on account of the acceleration of the surrounding fluid. Therefore, the hydrodynamic moment of inertia per unit length amounts to

$$J'' = 0.285 \cdot \frac{1}{6} \rho (2b)^4$$

[The moment of inertia of a parallelepiped with side a rotating about the center of gravity (Hütte I, 26th edition, p. 247) $J = \rho \frac{a^4}{6} L$]

or

$$J'' = 0.242 \pi \rho b^4$$

By the analytical method we found*

$$J'' = 0.234 \pi \rho b^4$$

which is equivalent to a mass increase of 27.6 percent. The agreement must be regarded as amazingly good.

In addition, Abell carried out tests with bilge keels along the longitudinal edges of the parallelepiped. The keels extended over the entire length and the ratio of the height of the keels to half the side of the square section (d/b) was 0.167. For this form Abell found an increase of the apparent moment of inertia of 72 percent compared with the value obtained by oscillating the same body in air, where the density of the body is set equal to that of the water. By means of a simple calculation we find that the increase of the hydrodynamic additional moment of inertia due solely to the bilge keels amounts to no less than 152.5 percent of the value found for the square without keels. On the basis of the theory, we would have expected an increase of only 127 percent (see Table 3).

*For the case of the square, the theoretical solution was already given by Proudman.²⁰ From Proudman's calculation it follows that J'' is equal to $0.232 \pi \cdot \rho \cdot b^4$.

Among the results of this comparison between theory and experiment three things are noteworthy:

1. The very considerable increase of the apparent moment of inertia, even by the addition of bilge keels that are not very high, is confirmed by experiment.

2. The good agreement between theory and experiment. It should be noted, moreover, that this good agreement exists in spite of angular forms which produce separation, in spite of large angles of oscillation (up to 30 degrees) and in spite of relatively low-frequency oscillations (i.e., slow motions, frequency about 1/3 hertz).

3. The measured hydrodynamic moments of inertia are greater than those calculated by theory.

Thus, for ship vibrations of all kinds, corrections not only for the hydrodynamic masses, but also for the hydrodynamic moments of inertia can be introduced into the calculations with a good degree of approximation.

IV. EFFECTS OF THE FREE SURFACE, LIMITED DEPTH, FREQUENCY, AND MOTION OF ADVANCE ON HYDRODYNAMIC MASS AND HYDRODYNAMIC MOMENT OF INERTIA

19. INFLUENCE OF A FREE SURFACE

In all of the investigations described thus far, the cross sections were surrounded on all sides by fluid. For problems of ship theory, however, it is important also to know the effect of a free surface on hydrodynamic masses and on hydrodynamic moments of inertia.

The boundary condition for the pressure at the free surface is $p = \text{constant}$. The motion is assumed to be irrotational and to possess a potential. Then for a fixed coordinate system the general Bernoulli equation [3] for flows which include static forces but neglect values of the square of velocities reads

$$\frac{p}{\rho} = -\frac{\partial \varphi}{\partial t} - g y + F(t)$$

Since the pressure is constant, the following relation holds for a particular time t and a surface elevation designated by η :

$$-\frac{\partial \varphi}{\partial t} = g \eta + \frac{p}{\rho} + \text{const}$$

$$\eta = -\frac{1}{g} \left[\frac{\partial \varphi}{\partial t} \right]_{y=\eta} + \text{const}$$

If we assume the surface elevation to be small, we may write

$$\eta = -\frac{1}{g} \left[\frac{\partial \varphi}{\partial t} \right]_{y=0}$$

where the constant is included in φ . The error introduced by defining the derivative at $y = 0$ is kept within the limits of the order of magnitude to be neglected. The consequence of limiting ourselves to small wave heights, will be that the angle $\frac{\partial \eta}{\partial x}$ which the surface makes with the horizontal will remain small. The condition to be satisfied that normal component of the fluid velocity at the free surface must equal the normal component of the velocity of the surface itself, thus yields the relation

$$\frac{\partial \eta}{\partial t} = \left[\frac{\partial \varphi}{\partial y} \right]_{y=0}$$

By eliminating η at $y = 0$ we obtain from the last two equations

$$\frac{\partial^2 \varphi}{\partial t^2} + g \frac{\partial \varphi}{\partial y} = 0$$

We now assume that the surface is to undergo wave motions. For the case of a simple harmonic oscillation of the fluid with the time factor $e^{i(\delta t + \epsilon)}$ * the following condition must be satisfied:

$$\sigma^2 \varphi = g \frac{\partial \varphi}{\partial y} \quad [67]$$

Up to this point, the ideas set forth were essentially in line with those given by Lamb (see Chapter IX).

If we now write the condition at the surface

$$\varphi = \frac{g}{\sigma^2} \cdot \frac{\partial \varphi}{\partial y} \quad [68]$$

and if we first consider oscillations of high frequency, then the expression on the right side becomes small and we obtain an approximation if we set $\phi = 0$.

Moullin¹⁹ has experimentally determined the flow about a parallelepiped oscillating at high frequency normal to the free surface by means of photographs, see Figure 42. It is clear from the streamlines which impinge normal to the surface that the surface indeed constitutes a potential line.

Moreover, the condition $\phi = 0$ is satisfied for heaving oscillations in a direction normal to the water surface (see Figure 17 where *DE* represents the surface) and likewise for rotation oscillations for which the axis of rotation lies at the surface (see Figure 35 where *AB* represents the surface). It is possible, therefore, to apply the results obtained above for a medium

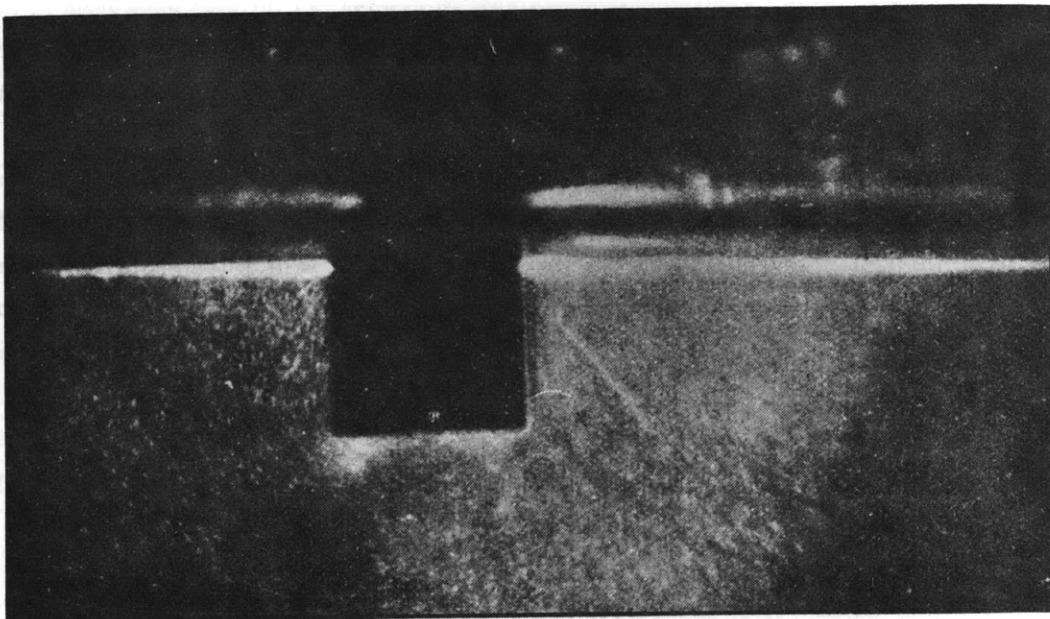


Figure 42 - Photograph of the Flow Pattern, by Moullin

* σ = circular frequency, ϵ = phase angle.

unlimited in all directions directly to these cases. It is true that at first this condition holds true only for high-frequency oscillations such as those which occur as elastic vibrations of ships. For low frequencies—which are important in general oscillations of the ship as a rigid body in the surrounding medium—a dependence of the oscillations on the frequency appears. In the vicinity of the ship there are generated standing waves as well as progressive waves of various sizes which depend upon the exciting frequency. The progressive waves produce an energy loss which together with the friction causes a damping of the oscillations. In the frequency range in which the standing waves show relatively large amplitudes, the kinetic energy of the flow in the vicinity of the oscillating body also assumes a greater value and vice versa. Hence, in the frequency ranges of large standing waves there is an increase of the hydrodynamic mass. A more detailed investigation of these phenomena would lead us far afield into the theory of surface waves. A comparison between the experimental results (Figure 32) and those calculated for an unlimited medium, values which at high frequency were found to apply even for bodies which move normal to the surface, show that we can expect the following result which is important for our purposes: the variations in magnitude resulting from frequency dependence become less important than the absolute value of m'' and hence may be disregarded in so far as the accuracy needed for determining ship vibrations is concerned. Let us point out also that the variation with frequency becomes smaller, the greater the depth of immersion of the parallelepiped as compared to its width, i.e., the greater the distance of the center of pressure is from the surface (see Figure 32). It would seem that we are justified in applying this line of reasoning to the case of rotational vibrations. Thus, in actual practice for both of these cases, we simply assume an infinite medium and take half the value of the hydrodynamic mass or the hydrodynamic moment of inertia of the double cross section, obtained by reflection in the free surface. The pressure distributions are likewise those already computed in Sections 3, 5, and 13 above.

For the case of horizontal oscillations in the direction of the water surface where waves are also generated, $\phi = 0$ is likewise the condition to be satisfied at the surface. Also with these oscillations, for which the author knew of no experimental investigations, we expect standing and progressive waves to be generated as well as a variation of the auxiliary hydrodynamic quantities with frequency. Nevertheless, here also we may assume that the condition $\phi = 0$ at the surface will satisfy actual conditions better and better with increasing frequency. It is to be noted, however, that for this case the solutions obtained for translational motions in Part II cannot be used since the boundary conditions to be satisfied are now different; when a free surface is present, the motions perpendicular and parallel to the surface are no longer mathematically equivalent.

If we limit ourselves to the parallelepiped, the first step to be taken will be to find the potential for the quadrant of the z -plane for which the boundary conditions shown in Figure 43 hold. A solution for this case may again be obtained by mapping an auxiliary t -plane into the z -plane and into a suitable half-strip of the ζ -plane (see Figure 44). The t -plane is

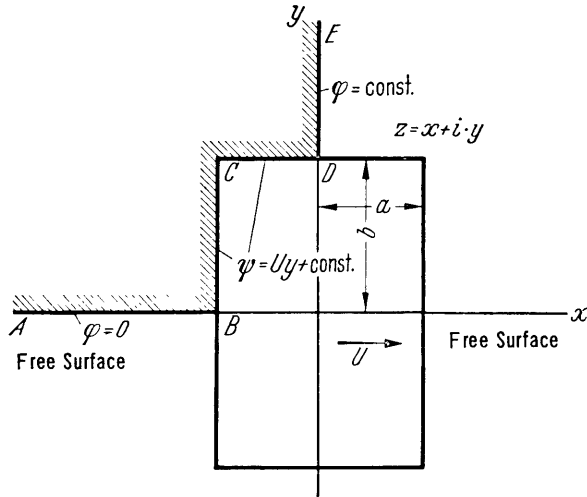


Figure 43 - Parallelepiped in the Surface

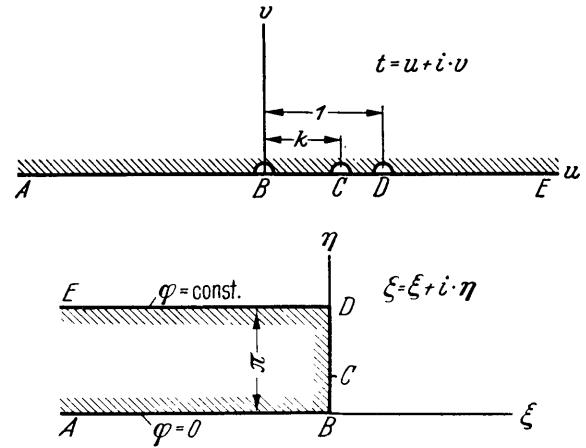


Figure 44 - Mappings for Horizontal Oscillations at a Free Surface

mapped into the z -plane by means of the transformation

$$z = c \int_0^t (-t)^{-\frac{1}{2}} (k-t)^{\frac{1}{2}} (1-t)^{-\frac{1}{2}} dt + c' \quad [69]$$

with $c' = -a$ and $c = \frac{ib}{k}$.

The aspect ratio is found to be

$$\frac{a}{b} = \frac{1}{k} \quad [70]$$

The transformation for mapping the t -plane into the ζ -plane is

$$\zeta = h \operatorname{arc} \cosh (1-2 t) + h' \quad [71]$$

with

$$h = 1 \quad \text{and} \quad h' = 0$$

These transformations have already been investigated in detail in Equations [30], [31], [32], [33], and [60]. By developing \int_0^t / \int_0^k into a cosine series for the half-strip we again obtain the kinetic energy for two quadrants

$$2 T = \pi \rho U^2 b^2 (a_1^2 + 2 a_2^2 + \dots + n a_n^2)$$

and the hydrodynamic mass is found to be

$$m'' = \pi \rho b^2 (a_1^2 + 2a_2^2 + \dots + na_n^2)$$

Thus, for the square cross section of length $2b$ immersed to a depth b , we obtained

$$m'' = 0.254 \cdot \pi \rho b^2$$

Previously (Section 11), for a square cross section of length $2b$ moving in a medium infinite in all directions, we obtained

$$m'' = 1.512 \pi \rho b^2$$

or $m'' = 0.756 \pi \rho b^2$ for two quadrants. Thus the ratio of the hydrodynamic mass of a body moving parallel to the free surface to its value in an infinite medium is 0.337.

The rectangular cross section moving horizontally in the direction of the free surface was also investigated experimentally by Koch, by use of an electrical analogue (see Figure 12). From Koch's experiment with the square we obtain the value 0.286 for the ratio of the hydrodynamic mass moving in the direction of the surface to its value in an unbounded medium.

In a manner similar to that described previously in Section 13 for cross sections surrounded by the fluid on all sides, it is also possible to determine the acceleration pressures for the case of the parallelepiped at the surface oscillating in the direction of the surface. Written in nondimensional form, we obtain

$$\frac{P_B}{\rho b \dot{U}} = \frac{1}{\rho b} \cdot \frac{dm''}{dy} = \frac{2 \int_0^k}{\sin \eta} \frac{1}{(-t)^2} \frac{1}{(1-t)^2} \sum_{n,m=1}^{n,m=\infty} a_n \sin n \eta \ m a_m \sin m \eta \quad [72]$$

For the case of the half-submerged parallelepiped, the calculation yields the pressure distribution indicated in Figure 45. At the surface the acceleration pressure must be zero because of the condition $p = \text{constant}$. The point of application of the resultant of pressure lies at a distance of $y = -0.568 b$ from the surface.

For the same ratio of width at waterline to depth of immersion, bodies of different cross-sectional shapes probably show a decrease in hydrodynamic mass due to the free surface of approximately the same magnitude as the square.

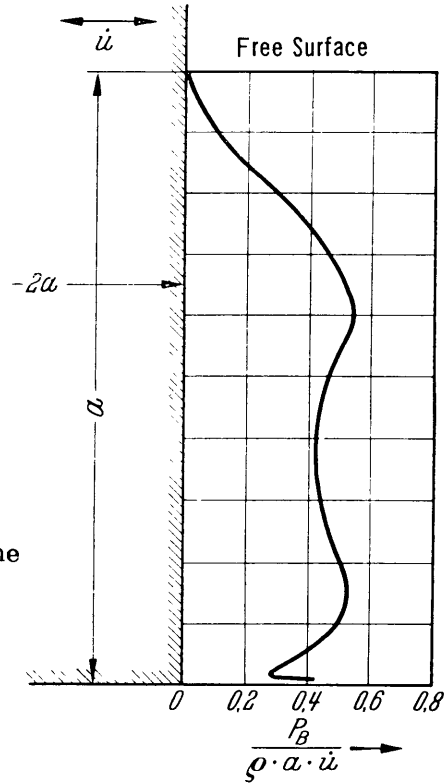


Figure 45 - Pressure Distribution of a Parallelepiped Oscillating in the Direction of the Free Surface

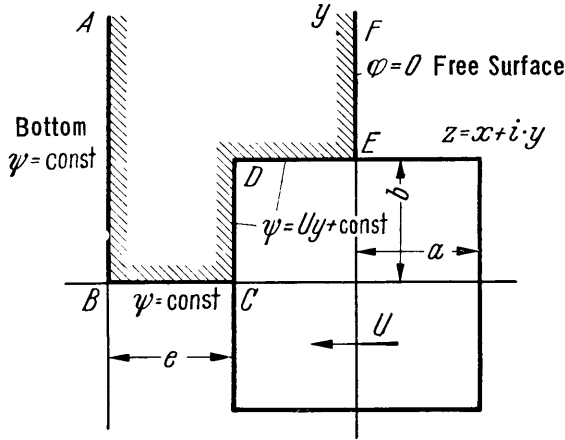


Figure 46 - Heaving Oscillations for the Case of Limited Depth and a Free Surface

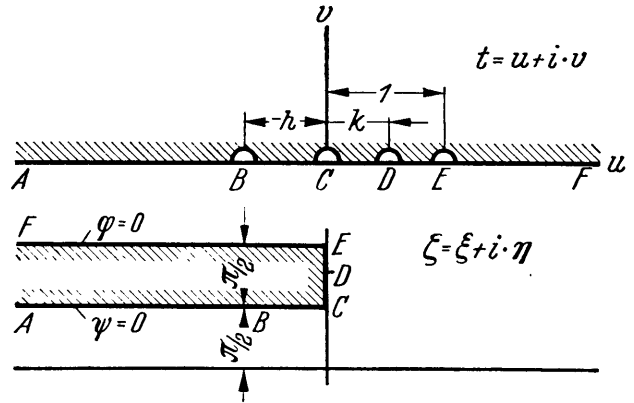


Figure 47 - *t*-Plane and ζ -Plane in Reference to Figure 46

20. EFFECT OF FINITE DEPTH

Any boundary in the fluid formed by a limited depth or side walls (quay walls, for instance) is sure to have an effect on the flow and consequently on the hydrodynamic masses, the hydrodynamic moment of inertia and the distribution and magnitude of the acceleration pressures. Our investigation in this connection will be confined to the case of a parallelepiped in a medium of limited depth oscillating in a direction perpendicular to the rigid bottom (see Figure 46). We shall include the effect of a free surface which is no longer mathematically equivalent to the case of the parallelepiped oscillating in an unbounded medium. In the absence of a free surface the line *EF* cannot be a potential line due to the asymmetry of the field around the parallelepiped with respect to the *y*-axis.

The auxiliary *t*-plane and the half-strip in the ζ -plane are represented in Figure 47. The transformation for mapping the *t*-plane into the *z*-plane is

$$z = c \int_0^t (-h - t)^{-\frac{1}{2}} (-t)^{-\frac{1}{2}} (k - t)^{\frac{1}{2}} (1 - t)^{-\frac{1}{2}} dt + c' \quad [73]$$

with $c' = -a$ and $c = \frac{ib}{k}$, $\frac{e}{b} = i \frac{\int_0^{-h} dt}{\int_0^1 dt}$ for the ratio of the depth below the bottom of the parallelepiped to its half-width and $\frac{a}{b} = -\frac{i \int_0^1 dt}{\int_0^1 dt}$ for the aspect ratio. If we again con-

fine our numerical calculations to the case of a square section, we have as a necessary condition to be satisfied

$$i \int_k^1 = \int_0^k \quad [74]$$

The mapping of the t -plane into the ζ -plane has already been dealt with before (see Section 11). We finally obtain once more the hydrodynamic mass

$$m'' = \frac{\pi}{2} \rho b^2 (a_1^2 + 2a_2^2 + \dots + na_n^2) \quad [75]$$

In the numerical calculation for the square it is first of all necessary that the relation [74] for an arbitrarily prescribed h be fulfilled which can be done only by repeated choices of k and by graphic integration and interpolation. From Equation [73], it is seen that for a different h , for a different depth under the bottom e , a different value of k is obviously needed to satisfy the condition [74] so that the interpolation process must be repeated for each value of h chosen. The calculations involved were carried out without great accuracy; the cosine series, for instance, was limited to six terms. In this manner we obtained Table 4.

The percentage increase of C was determined in comparison to its value for the parallellepipid oscillating in unlimited water. The results obtained are in good agreement with those found by Koch by means of the electrical experiment. For application of these results, we call the reader's attention especially to the data plotted in Figures 11 and 12.

TABLE 4

e/b	m''	C	Percentage Increase of C
∞	$1.51 \frac{\pi}{2} \cdot \rho \cdot b^2$	1.51	0
2.565	$1.67 \frac{\pi}{2} \cdot \rho \cdot b^2$	1.67	≈ 11
1.78	$1.77 \frac{\pi}{2} \cdot \rho \cdot b^2$	1.77	≈ 18

21. EFFECTS OF FREQUENCY AND ADVANCE

The effect which the frequency of the oscillations has on the hydrodynamic masses and moments of inertia has already been discussed repeatedly in connection with wave formation in a free surface. A certain dependency on frequency resulting from the appearance of vortices must be added to this, because vortices require a certain amount of time for their formation and are likewise affected by the periodicity of the motion. It may also be assumed in this case that rapid oscillations produce a flow in the real fluid which may be closely approximated by potential flow.

It is to be expected that the results obtained by calculation are affected by the presence of a boundary layer on the surface of the oscillating body, though this effect is kept within very moderate limits due to the small thickness of this layer.

The objection raised occasionally that the added hydrodynamic masses calculated for a ship which is rolling or vibrating with no translatory motion do not apply to the case of a ship underway is unfounded. If the speed of advance is assumed to be constant, obviously

no hydrodynamic mass has to be added either in the direction of advance or in the opposite direction; hence, the values calculated at right angles to the direction of advance represent the entire hydrodynamic mass. At most, perhaps a slight effect could be expected to result from a variation of the vortex formation and the boundary layer and also from the generation of waves. It is presumed that as long as the speed of advance is moderate, i.e., as long as no great change occurs in the surface due to the generation of waves, the ship motion is favorable rather than unfavorable for the potential flow representation on which our calculation is based. It has been confirmed by experiment again and again that while the damping of oscillations is largely dependent upon the speed of advance, the periods of rolling and elastic oscillations measured with or without any speed of advance are practically the same.

V. APPLICATIONS OF THE HYDRODYNAMIC MOMENTS OF INERTIA

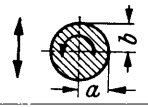
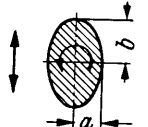
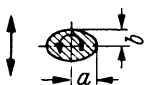
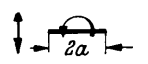
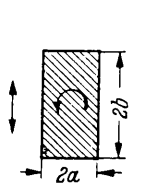
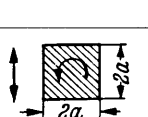
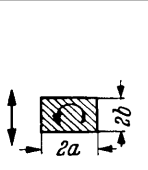
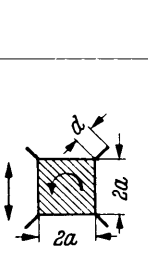
22. TABULATION OF THE AVAILABLE VALUES. ADDITIONAL CALCULATIONS.

Figures 10 and 48 contain just about all the values for the hydrodynamic masses and hydrodynamic moments of inertia that have been calculated for two-dimensional motion up to now. With these values a good many problems of the ship theory in which accelerations or decelerations play a part can be dealt with quite accurately. Three-dimensional flow about a solid may be determined by means of Lewis's coefficients of reduction (see Figure 5).

By the previously described method for the calculation of the added hydrodynamic quantities, practically all angular cross sections can be handled. We can now replace every curve or every transverse section by a number of straight line segments which make it amenable to calculation. At the suggestion of Professor Horn, one of his assistants, Dipl. Ing. Fatur, undertook this work for a trawler in 1942. Unfortunately, this work which had already progressed quite far was destroyed in an air raid. I should like to express my appreciation to Professor Horn as well as to Professors Weinblum and Ebner for making a number of suggestions and for giving me their encouragement in the pursuit of my investigations.

23. APPLICATION TO ELASTIC OSCILLATIONS

A satisfactory pre-determination of the natural frequency of the vertical flexural vibrations, also called elastic oscillations or vibrations, is possible only by increasing the mass of the ship by the hydrodynamic mass. The mathematical data for such a determination of the hydrodynamic mass was given by Lewis in 1929 and has been discussed by Professor Horn in his lectures ever since that time. Lewis proceeds as follows: To the weights of the ship plus its cargo, the "weight of the hydrodynamic mass" must be added. The hydrodynamic mass is determined by means of the inertia coefficients C given by Lewis for curves similar to transverse sections. Thus, the ship hull is considered as being made up of cylindrical segments of different transverse sections, each of which is assigned an inertia coefficient C obtained by comparing the given contour with Lewis's curves. Then we multiply by $1/2 g R$ (We multiply by $1/2$ because a free surface exists, i.e., because only half of the double cross section on which the calculation is based is submerged; by g in order to obtain a "weight curve of the hydrodynamic mass," and finally by the coefficient of reduction R for two nodes (see Figure 5) in order to take account of the three-dimensional flow about the solid.) Thus we obtain the bell-shaped curve in Figure 49 which resembles the displacement curve. (Incidentally, the displacement curve might be used as a first approximation.) The area under the curve, "weight of the hydrodynamic mass," represents the weight of the entire added mass. In the case of this ship, the latter is greater than the weight of the ship itself (1650 tons as compared to 1360 tons).

Cross-Sectional Forms		Hydrodynamic Mass per Unit Length	Inertia Coefficient $C = \frac{m''}{m'' \text{ circle}} =$	Hydrodynamic Moment of Inertia per Unit Length	Inertia Coefficient for Rotation $D'' = \frac{J''}{J'' \text{ plate}} =$	
Direction of Motion	Axis of Rotation					
	$\frac{a}{b} = 1$ (circle)	$m'' = \pi \rho a^2$ ^[1]	1	$J'' = 0$	0	
		$m'' = \pi \rho a^2$ ^[1]	1	* $= 0.125 \pi \rho (a^2 - b^2)^2$ ^[1]	$\left[\left(\frac{b}{a} \right)^2 - 1 \right]^2$	
						
	Plate	$= \pi \rho a^2$ ^[1]	1	$= 0.125 \pi \rho a^4$ ^[1]	1	
	$\frac{a}{b} = \frac{1}{2}$	$= 1.7 \pi \rho a^2$ ^[2]	1.7	$= 0.15 \pi \rho b^4$ ^[5]	} 1.2 } Referred to Plate of Width 2b	
	$\frac{a}{b} = \frac{1}{5}$	$= 1.98 \pi \rho a^2$ ^[2]	1.98	$= 0.15 \pi \rho b^4$ ^[5]		
	$\frac{a}{b} = \frac{1}{10}$	$= 2.23 \pi \rho a^2$ ^[2]	2.23	$= 0.147 \pi \rho b^4$ ^[5]		
	Square	$= 1.51 \pi \rho a^2$ ^[2]	1.51	$= 0.234 \pi \rho a^4$ ^[3, 5]	1.872	
	$\frac{a}{b} = 2$	$= 1.36 \pi \rho a^2$ ^[2]	1.36	} $= 0.15 \pi \rho a^4$ ^[5] }	} 1.2 } Referred to Plate of Width 2a	
	$\frac{a}{b} = 5$	$= 1.21 \pi \rho a^2$ ^[2]	1.21			
	$\frac{a}{b} = 10$	$= 1.14 \pi \rho a^2$ ^[2]	1.14			$= 0.147 \pi \rho a^4$ ^[5]
	$\frac{d}{a} = 0.05$	$= 1.61 \pi \rho a^2$ ^[5]	1.61	} $= 0.31 \pi \rho a^4$ ^[5] }	} 2.4 } Referred to Plate of Width 2a	
	$\frac{d}{a} = 0.1$	$= 1.72 \pi \rho a^2$ ^[5]	1.72			} $= 0.4 \pi \rho a^4$ ^[5] }
	$\frac{d}{a} = 0.25$	$= 2.19 \pi \rho a^2$ ^[5]	2.19			

*Translators note: This expression, which was incorrect in the original copy, has been corrected for the translation.

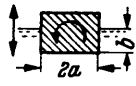
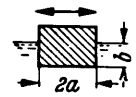
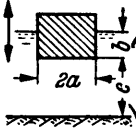
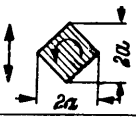
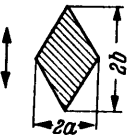
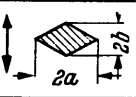
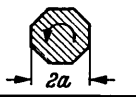
Cross-Sectional Forms		Hydrodynamic Mass per Unit Length	Inertia Coefficient $C = \frac{m''}{m''_{\text{circle}}} =$	Hydrodynamic Moment of Inertia per Unit Length	Inertia Coefficient for Rotation $D'' = \frac{J''}{J''_{\text{plate}}} =$
Direction of Motion	Axis of Rotation				
	$\frac{a}{b} = 1$	^[2] $= 0,75 \pi \rho a^2$ $= \frac{1}{2}$ square	0.75	^[5] $= 0.117 \pi \rho a^4$	0.936
	$\frac{a}{b} = 1$	^[5] $= 0,25 \pi \rho a^2$	0.25		
	$\frac{e}{b} = \infty$	^[5] $= 0.755 \pi \rho a^2$	0.75		
	$\frac{e}{b} = 2.6$	^[5] $= 0.83 \pi \rho a^2$	0.83		
	$\frac{e}{b} = 1.8$	^[5] $= 0.89 \pi \rho a^2$	0.89		
	$\frac{e}{b} = 1.5$	^[6] $\approx 1 \pi \rho a^2$	≈ 1		
	$\frac{e}{b} = \frac{1}{2}$	^[6] $\approx 1.35 \pi \rho a^2$	≈ 1.35		
	$\frac{e}{b} = \frac{1}{4}$	^[6] $\approx 2 \pi \rho a^2$	≈ 2		
		^[2] $= 0.76 \pi \rho a^2$	0.76	^[5] $= 0.059 \pi \rho a^4$	0.47
	$\frac{a}{b} = \frac{1}{2}$	^[2] $= 0.67 \pi \rho a^2$	0.67		
	$\frac{a}{b} = \frac{1}{5}$	^[2] $= 0.61 \pi \rho a^2$	0.61		
	$\frac{a}{b} = 2$	^[2] $= 0.85 \pi \rho a^2$	0.85		
	Regular Octagon			^[4] $\approx 0.055 \pi \rho a^4$	0.44

Figure 48 - Tabulation of Hydrodynamic Masses, Hydrodynamic Moments of Inertia, and Inertia Coefficients As Calculated by [1] Lamb, [2] Lewis, [3] Proudman, [4] Weinblum, [5] Wendel, [6] Determined Experimentally (Electrical Analogue) by Koch

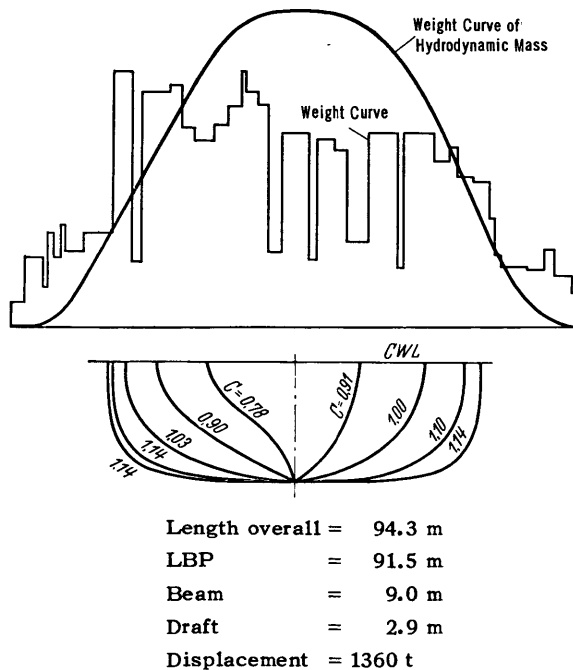


Figure 49 - "Weight Curve" of the Hydrodynamic Mass

The inclusion of this added weight therefore more than doubles the weight of the ship. The frequency at which a bar oscillates decreases as its mass increases. Doubling the mass gives a reduction in frequency by a factor $\frac{1}{\sqrt{2}} = 0.7$. An accurate treatment of the vibration calculation does not usually give exactly this value for the reduction factor because the mass distribution over the length changes also. In the resulting curve, representing the weights of the ship plus the weights of the hydrodynamic masses, the weight is concentrated more toward the middle of the ship, which again increases the frequency somewhat. The nodes also move more toward the middle which produces greater amplitudes at the stern and bow. Comparisons between measured periods and those calculated by this method show very good agreement.

Bilge keels having a height of $1/40$ of the (ship) width bring about an increase of the added mass of about 6 percent. Consequently, the frequency is thereby reduced by about 3 percent.

In the case of horizontal flexural vibrations, the hydrodynamic mass to be added amounts to only about $1/3$ of that needed in the case of the vertical flexural vibrations. The total mass therefore is considerably less; the elastic restoring forces, on the other hand, are greater because the moment of inertia, referred to the vertical axis, is greater in most cases. Hence, horizontal vibrations will be executed at a considerably higher frequency. This has been confirmed by measurements. Likewise for torsional vibrations, the hydrodynamic component to be added is considerably smaller than it is for vertical flexural vibrations. With these two types of vibrations, bilge keels will also reduce the frequency to some extent.

24. APPLICATION TO HEAVING

The effect of the hydrodynamic mass on heaving is similar to its effect on the vertical flexural vibrations. The period of heaving oscillations of the whole ship regarded as a rigid body is proportional to the square root of the entire oscillating mass. Here as in the case of flexural vibrations there is a hydrodynamic component to be determined which differs from the other in that the coefficient of reduction for heaving oscillations must be used. Here also is to be expected an approximate doubling of the mass and consequently an increase in the period by a factor of $\frac{\sqrt{2}}{1} \approx 1.4$ or about 40 percent. Bilge keels increase the period by about the same percent as in the case of flexural vibrations.

25. APPLICATION TO THEORY OF ROLLING

Until very recently, the theory of rolling was based on the assumption that though the fluid had the property of buoyancy, it had neither mass nor viscosity. All research workers, including Daniel Bernoulli, W. Froude, Bertin, Kriloff, etc., until recently followed the example of Euler, the founder of ship dynamics and the first to treat the free vibration of ships in his work, "Scientia Navalis," published in 1749.

In 1861, W. Froude not only developed his well-known theory of rolling in a seaway which took the form of the exciting surface waves into consideration, but he also pointed out that corrections are necessary in the equation for the rolling motion and indicated the numerical values to use.⁴ In accordance with this, two corrections are required:

1. An apparent moment of inertia which considerably exceeds the calculated moment of inertia of the rigid ship.
2. A term which summarily takes into account the damping of the oscillations due to wave and vortex formation as well as friction.

In a fundamentally analogous manner successors of W. Froude (especially Bertin, Kriloff and R.E. Froude) also dealt with the rolling motion and the general oscillations of a ship considered as a rigid body (Kriloff).

A number of problems, some of which are important, cannot be solved, however, if the forces due to inertia and viscosity are neglected, for example: the magnitude of the apparent masses and apparent moments of inertia which actually determine the period of oscillation, the location of the instantaneous axis of rotation about which the rolling motions occur, the effect of changes in form of the submerged portion of the ship on the natural period, etc. In more recent times, investigators have undertaken to introduce these forces into the differential equation of free rolling, not only in the form of correction terms or correction factors to be determined empirically, but also as hydrodynamic terms to be added to the dynamic terms. In doing so, however, they at first confined themselves to very particular floating bodies. Baumann,²³ for instance, investigates the motions of the circular cylinder, taking into account the hydrodynamic inertia forces and viscosity forces, while Brard¹¹ treats the elliptic cylinder, taking the hydrodynamic inertia forces into consideration.

In the following discussion, we shall indicate several formulas by which the effect of the hydrodynamic inertia forces can also be determined for cross sections which more closely approximate actual ship forms.

We consider a body at the surface whose mass distribution though not homogeneous is symmetrical with respect to the y -axis (see Figure 50)* and we wish to calculate its center

*In view of the example treated at the end of this section, a rectangle has been used as the cross section of the body in Figure 50.

of rotation and apparent moment of inertia for small oscillations neglecting the dissipation of energy. We make use of the following notations given in Figure 50:

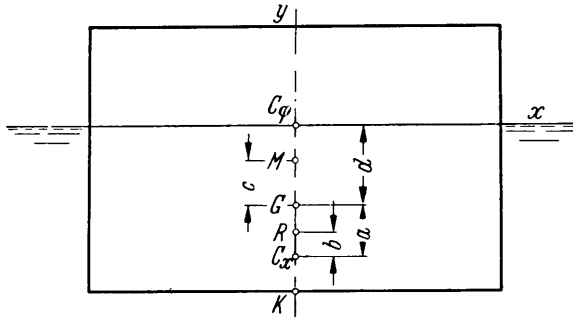


Figure 50 - Free Rolling Motions in an Inviscid Fluid

- M the metacenter,
- G the center of gravity,
- C_x the point of application of a single force in the x -direction which results from the hydrodynamic water mass,
- C_ϕ the geometric center of the rectangular section consisting of the cross section under water and its reflected image in the water surface (thus this point always lies on the surface of the water),
- R the "apparent" center of mass (center of rotation in the absence of dissipation forces).

The distances c , d , a , and b are to be taken positive if the points M , G , C_ϕ , C_x , and R are located in the order shown. If G lies above the water line, then d becomes negative, and similarly a becomes negative when C_x lies above G .

The kinetic energy of a rigid body moving both in translation and in rotation about R from its initial position is

$$2T = m (\dot{x}_R^2 + \dot{y}_R^2) + [J_G + m (a-b)^2] \dot{\phi}^2 \quad [76]$$

In order to determine the kinetic energy imparted to the flow by a solid body moving in translation and rotation, we first calculate the momentum and moment of momentum vectors for the motion produced by the combined effects of translation and rotation. The momentum of the translational motion becomes

$$\mathfrak{S} = m_x'' \dot{x} + m_y'' \dot{y} \quad [77]$$

where \dot{x} and \dot{y} denote the velocity of any arbitrary point on the body. The moment of momentum for rotation about C_ϕ becomes

$$\mathfrak{S} = J_c'' \dot{\phi} \quad [78]$$

In Equations [77] and [78] m_y'' and J_c'' represent, respectively, half the hydrodynamic masses and hydrodynamic moments of inertia of the double body which includes the portion formed by reflection in the water surface; m_x'' is the hydrodynamic mass applicable to motion at and parallel to the free surface.

The free motion from a heeling position would correspond to a rotation of a massless rigid body about a point C_x . The momentum for this motion is given by [77] while the moment of momentum assumes the value

$$\mathfrak{S} = [J_c'' - m_x'' (a + d)^2] \dot{\varphi} \quad [79]$$

For rotation about another point on the symmetry axis it is necessary to add another moment of momentum for the hydrodynamic mass m_x'' considered to act at the point C_x ; thus we obtain

$$\mathfrak{S} = [J_c'' - m_x'' (a + d) + m_x'' b^2] \dot{\varphi} \quad [80]$$

The kinetic energy of the motion consisting of the translation of R and rotation about R , is obtained from the scalar product of the momentum quantities and the corresponding velocities:

$$2T'' = m_x'' \dot{x}_R^2 + m_y'' \dot{y}_R^2 + J_c'' \dot{\varphi}^2 - m_x'' (a + d)^2 \dot{\varphi}^2 + m_x'' b^2 \dot{\varphi}^2 \quad [81]$$

For the total kinetic energy of the conservative system consisting of the rigid body and the surrounding fluid, we obtain by adding [76] and [81]

$$2T' = 2T + 2T'' = (m + m_x'') \dot{x}_R^2 + (m + m_y'') \dot{y}_R^2 + (J_G + J_c'') \dot{\varphi}^2 + m (a-b)^2 \dot{\varphi}^2 - m_x'' (a + d)^2 \dot{\varphi}^2 + m_x'' b^2 \dot{\varphi}^2 \quad [82]$$

The kinetic energy for free rotation of the entire system must be a minimum; this includes motions arising from external moments provided the moment vector is free. Since b is the only free variable in [82] (R must obviously lie on the axis of symmetry), the differential quotient

$$\frac{dT'}{db} = -m(a-b) + m_x'' b$$

must vanish at the center of rotation. Hence it follows that

$$b = \frac{m}{m + m_x''} a \quad [83]$$

whereby the center of rotation R for the conservative system is determined since the positions of C_x and G are known.

In order to calculate the apparent moment of inertia, we introduce the expression [83] for b into the relation for the kinetic energy [82]. Then the total kinetic energy of the body rotating about R becomes

$$2T' = (m + m_x'') \dot{x}_R^2 + (m + m_y'') \dot{y}_R^2 + (J_G + J_c'') \dot{\varphi}^2 + \frac{m m_x''}{(m + m_x'')} a^2 \dot{\varphi}^2 - m_x'' (a + d)^2 \dot{\varphi}^2 \quad [84]$$

The potential energy of the heeling and heaving ship is

$$2 U = m g c \varphi^2 + \gamma B y^2 \quad [85]$$

(B = ship breadth, c = metacentric height.)

Since the moments of the masses and moments of inertia are divided by L on account of the two-dimensionality, so has the second term in [85] been divided by the length L .

By means of the general form of the Lagrange equation of motion

$$\frac{d}{dt} \left(\frac{\partial T}{\partial \dot{q}_i} \right) - \frac{\partial}{\partial q_i} (T - U) = 0 \quad [86]$$

in which the q_i -quantities represent the generalized* coordinates while T and U denote the kinetic and potential energy of the entire system (here, $T = T'$), we now set up the equations of motion in generalized coordinates which for this case are obviously x , y , and ϕ . Thus we obtain the following relations:

$$(m + m''_x) \ddot{x}_R = 0 \quad [87]$$

from which it follows that no transverse oscillation occurs.

$$(m + m''_y) \ddot{y}_R + \gamma B y = 0 \quad [88]$$

for the heaving oscillation, wherein the mass must be increased by the hydrodynamic mass of water for motion in the y -direction. Finally

$$\left[J_G + J''_c + \frac{m m''_x}{m + m''_x} a^2 - m''_x (a + d)^2 \right] \ddot{\varphi} + m g c \varphi = 0 \quad [89]$$

from which the apparent moment of inertia J' for the rolling oscillation takes on the value

$$J' = J_G + J''_c + \frac{m m''_x}{m + m''_x} a^2 - m''_x (a + d)^2 \quad [90]$$

The terms following the first term J_G , taken together, represent the added hydrodynamic moment of inertia.

*Generalized coordinates are coordinates which can be varied independently of one another without violating the conditions to which the system is subject. As for the rest, we call the reader's attention to the comprehensive textbooks of Mechanics.

For the circular cylinder, we specifically obtain $J''_c = 0$ and $-a = c = d$; the apparent moment of inertia thus assumes the value

$$J' = J_G + \frac{m m''_x}{m + m''_x} a^2$$

which was already indicated by Baumann.²³

As illustration, the position of the center of rotation, the added hydrodynamic moment of inertia, and the apparent moment of inertia will now be calculated for a simple numerical example. The immersed part of the (infinitely long) floating body which is assumed to have the form of a parallelepiped is to represent one-half of a square. By reflection in the surface, therefore, a whole square is obtained. We furthermore assume that $\overline{MG} = c = \frac{1}{12} B$. For \overline{MF} * we obtain $\overline{MF} = \frac{B^2}{12T} = \frac{1}{6} B = 0.167 B$, thus $d = \overline{KC}_\phi - \overline{KG} = 0.167 B$. From Section 19, it follows that $a + d = 0.284 B$, or, with the value for d , $a = 0.117 B$, and for the hydrodynamic mass $m''_x = 0.0636 \pi \cdot \rho \cdot B^2$. From Section 16, we know that $J''_c = 0.117 \rho \frac{B^4}{16} = 0.023 \cdot \rho \cdot B^4$. With this, it follows from [83] for the location of the center of rotation R that $b = 0.714 a = 0.0835 B$. The center of rotation R thus lies $0.201 B$ below the waterline and $0.034 B$ below G . These distances have been plotted to scale in Figure 50. The added hydrodynamic moment of inertia amounts to

$$J'' = J''_c + \frac{m m''_x}{m + m''_x} a^2 - m''_x (a + d)^2$$

$$J'' = 0.00859 \cdot \rho \cdot B^4$$

With $J_G = m \cdot i^2$ and for $i = 0.35 B$, we obtain

$$J_g = \frac{\rho}{2} \cdot B^2 \cdot 0.123 B^2 = 0.0613 \cdot \rho \cdot B^4$$

For parallelepipeds having dimensions like a real ship, beam $B = 12 m$, draft $= 6 m$, C_x lies $3.40 m$ below the waterline and R lies $0.41 m$ below G if $\overline{KG} = 4 m$. The added hydrodynamic moment of inertia amounts to 14 percent of the moment of inertia of the rigid body referred to the axis passing through G ; the radius of gyration of the rigid body was assumed to be $0.35 B$ in this case. For models of merchant ships, Weinblum and Block obtained experimental values between 12 and 15 percent.

* F is the center of buoyancy for no angular displacement. From standard texts in Naval Architecture

$$\overline{MF} = \frac{\text{moment of inertia of the waterline area}}{\text{volume of displaced liquid}}$$

In expression [90] we found a relation which permits us to calculate the apparent moment of inertia. With the aid of the added hydrodynamic quantities indicated and the pressure distributions, the apparent moment of inertia can also be determined approximately for usual hull forms. To this end, the hull forms will be treated in the following manner: The body of the ship, in the longitudinal direction, is assumed to be composed of cylindrical elements whose length corresponds to the selected frame spacing and whose cross section is the transverse section at the middle of the element. The cylindrical elements are now conceived to be surrounded by a two-dimensional flow; hence, we can use the expressions for the hydrodynamic masses and moments of inertia derived in Parts II, III, and IV of this paper. If we are dealing with transverse sections which vary greatly from those treated before or in the available literature, the transverse section can be approximated by a polygon in most cases. The calculation of the hydrodynamic masses and moments of inertia can then be accomplished without any fundamental difficulty by following the method described in detail in Sections 11, 12, 16, 17, 19, and 20. The results are not affected materially by the corners which occur in this case. If approximations through the use of polygons are not satisfactory, it will be necessary to seek suitable transformation functions, by a method of trial and error, proceeding perhaps in the manner indicated in Sections 8 and 9. In the case where we are dealing with simple experimental bodies having the shape of parallelepipeds with an aspect ratio $B/T = 2$, the indicated values already suffice both for the hydrodynamic mass in translational motion in the direction of the surface and for the hydrodynamic moment of inertia, too.

On the basis of the investigations of Sections 12 and 17, the effect of bilge keels can likewise be taken into account without further calculation. Thus, with the aid of Figure 41, the percentage increase of the inertia coefficient D for a square section will be determined first. This percentage increase can also apply to underwater sections which do not vary too greatly from the half-submerged square. The hydrodynamic mass in translation in the direction of the surface can be determined in an entirely analogous manner; in this case, the percentage increase required because of the bilge keels will be added to the hydrodynamic mass which is already reduced because of the surface (see Section 19).

On account of the bilge keels, the point of application C_x is moved downward and thereby m_x'' and I_C'' become considerably larger. As a result of this, the center of rotation R also moves downward and the total added moment of inertia becomes larger. For the example (keel height 30 cm), R moves down about 25 cm and the added moment of inertia becomes approximately 16.5 percent of the moment of inertia of the rigid body. The often-observed increase of the period of roll by the presence of bilge keels is thereby explained. There is but a slight increase, however, since the hydrodynamic component of the moment of inertia is very small compared with the total moment of inertia.

For translation in the y -direction, the masses and moments of inertia calculated for the elementary cylinders are then to be multiplied by the coefficient of reduction R_1 , corresponding to the length-width ratio of the ship, and for translation in the x -direction and for

rotation away from the initial position, they are to be multiplied by a second coefficient of reduction R_2 , corresponding to the length-double draft ratio. Finally, the reduced values obtained for the individual cylindrical elements are to be summed up.

It remains to determine the point of application C_x of the hydrodynamic mass m_x'' . For the half-immersed square moving in translation in the direction of the surface, the point of application C_x was determined in Section 19. For other polygons, we have to use fundamentally the same procedure. For rough calculations, the point of application C_x can, in many cases, be estimated with good approximation with the aid of the calculated pressure distributions. In this connection, it should be noted, however, that for motion in the direction of the surface, the pressure at the surface must always be equal to zero. Moreover, it ought to be pointed out in particular that the pressures must always be normal to the surface of the body. From this it follows that for each circular segment of the underwater section, the point of application must lie at the center of curvature and that for the horizontal half-submerged ellipse, the point of application must lie above the water surface. The point of application of the entire hydrodynamic mass m_x'' for the whole length of the ship is then obtained by means of a simple moment equation.

26. EFFECT OF LIMITED DEPTH OF WATER ON ROLLING OSCILLATIONS AND ON VERTICAL FLEXURAL VIBRATIONS

A limited depth of water or a quay wall running close to the ship exert a similar influence on the period of roll as the bilge keels. Hereby, the hydrodynamic moment of inertia is increased and, indeed, quite considerably so under certain circumstances. The period becomes greater than that for the ship carrying the same load in open deep water. This is of importance if any conclusions are to be drawn from a rolling test with respect to the existing metacentric height. I'' may assume three to four times its value in open water. Let us assume four times the value, for example, which is somewhat extreme. In that case, the natural period will be about 1.15 times as great as in deep water. If we now calculate the metacentric height from this period measured by the clock, as is customary in rolling tests, then the metacentric height will be too small by about 30 percent. With this error we are on the safe side, however.

Particularly noteworthy is the effect of a limited depth of water on the frequency of the vertical flexural vibrations which has already been pointed out by Schnadel.^{25, 26} We have already seen that by taking the hydrodynamic mass into consideration the entire mass is, in general, more than doubled. If a ship with a draft of 8 m travels in water which is only slightly deeper, say 2 m of water under the keel which may occur at the mouths of rivers, its hydrodynamic mass will be tripled. The frequency is thereby reduced to about 0.7 of the original value; thus we have a reduction from say 100 oscillations per minute in open water to 70.

It is common knowledge that resonance occurs whenever the frequency of the vibration-exciting forces from the engine or propeller coincides with the natural frequency of the ship. Hence, if a ship's course is over a region of limited depth, the resonance frequency will

decrease quite considerably in some cases. Thus a ship which ordinarily travels along with practically no oscillations in deep water may be set into resonance vibration at a constant RPM of the engine by coming into shallow water.

REFERENCES

1. Lamb, H., "Lehrbuch der Hydrodynamik," translated from the 5th English edition by E. Helly, Leipzig (1931).
2. Wien, W., "Lehrbuch der Hydromechanik," Leipzig (1900).
3. Prandtl-Tietjens, "Hydro- und Aeromechanik," 2 Vols., Berlin (1929 and 1931).
4. Prandtl, L., "Führer durch die Strömungslehre," 3rd edition, Braunschweig (1949).
5. Froude, W., "On the Rolling of Ships," Transactions Institute of Naval Architects (1861).
6. Lewis, "The Inertia of the Water Surrounding a Vibrating Ship," Transactions Society of Naval Architects (1929).
7. Koch, "Eine experimentelle Methode zur Bestimmung der reduzierten Masse des mit-schwingenden Wassers bei Schiffsschwingungen," Ing. Arch. 4 (1933).
8. Durand, in Durand, "Aerodynamic Theory," Vol. 1, Berlin (1934).
9. Munk, in Durand, "Aerodynamic Theory," Vol. 1 and 6, Berlin (1934).
10. Weinblum, "Beitrag zur Theorie der Kursstabilität und Steuerfahrt," Schiffbau (1937), p. 51.
11. Brard, "Les effect de l'eau entrainee sur le mouvement de roulis en eau calm," Bull. de l'Ass. Techn. Mar. Aero., Paris (1939).
12. Havelock, "Waves Produced by the Rolling of a Ship," Philosophical Magazine VII, Vol. 29 (1940). In addition, articles in many annual publications of the Prod. Roy. Soc. A, London.
13. Wien-Harms, "Handbuch der Experimentalphysik," Vol. IV, 2nd Part, p. 385.
14. Holstein, "Untersuchungen an einem Tauchschwingungen ausführenden Quader," WRH. (1936), p. 385.
15. Schwarz, H.A., "Über einige Abbildungsaufgaben," Ges. Math. Abh., Vol. II, pp. 65-83.
16. Rothe-Ollendorf-Pohlhausen, "Funktionentheorie und ihre Anwendung in the Technick," Berlin (1931).
17. Biezeno-Grammel, "Technische Dynamik," Berlin (1939). On page 132, a clearly understandable scheme (diagram) of Runge's method will be found.
18. Nicholls, "Vibration of Ships," Transactions Institute of Naval Architects (1924).
19. Moullin, "Some Vibration Problems in Naval Architecture," Transactions of the 3rd International Congress for Applied Mechanics, Part III, Stockholm (1930).
20. Proudman, "Rotating Log of Square Section in an Infinite Fluid," Appendix to Reference 21.

21. Abell, "Experiments to Determine the Resistance of Bilge-Keels to Rolling," Transactions Institute of Naval Architects (1916), p. 80.
22. Weinblum, "Die Bewegungsgleichungen des Schiffes im Seegang," Schiffbau (1931), p. 529.
23. Baumann, "Schlingerversuch mit einem Kreiszyylinder," Schiffbau (1937), p. 371
24. Weinblum and Block, "Die Verlängerung der Schlingerperiode eines Frachtschiffs infolge der mitschwingenden Wassermasse," Schiffbau (1933), p. 285.
25. Schnadel, "Elastische Schwingungen bei Stapellauf der 'Caribia'," Jahrb. d. Schiffbautechn. Ges. (1935).
26. Schnadel, "Ergebnisse der Ablaufmessungen beim Stapellauf der 'Caribia'," Schiffbau (1935), p. 320.
27. Ebner, "Über Gleichgewicht und Bewegung der Seeflugzeuge bei Wind und Seegang," Jahrb. d. Luftfahrtforschung (1940), Vol. I, p. 640.

DISCUSSION

Professor H.E. Dickmann, Dr. Eng., Karlsruhe

The subject presented by the lecturer has a particular practical importance. The applicability of the results has been discussed at great length for the field of ship theory which includes ship motions and oscillations. Over and beyond this, however, the problem is also of particular significance for marine engineering. Wherever engine parts or surfaces of iron or other material come into contact with liquids and are apt to be set into vibration, the vibration of such structural parts can be predicted, hence the determination of their natural frequencies, above all, can be made with accuracy only if the associated hydrodynamic masses and moments of inertia are taken into consideration. The torsional vibrations generated by propeller shafts serve as an example in which not only the mass of the metal propeller, but also the hydrodynamic pressures of the surrounding water must be taken into account.

The pertinent literature on this subject is widely scattered and since the end of the war has frequently been inaccessible. The lecturer therefore deserves a great deal of praise for having compiled a survey of all relevant investigations on this problem and for having supplemented these by extensive calculations of his own.

To one of these recent contributions I should like to raise a modest objection. In the example of the body oscillating horizontally at the free water surface, a hydrodynamic pressure distribution has been plotted in Figure 45 which, decreasing slowly in an upward direction, reaches atmospheric pressure at the surface of the water. It is true that this limiting condition seems to be very plausible. I surmise, however, that in the case of transverse oscillations the resulting hydrodynamic pressures will have considerably greater amplitudes and that—in a first approximation at least—they will conform to the pressure pattern which would result in the case of a plane surface of separation with a reflected double body. It is true that the necessary limiting condition at the surface is at first not fulfilled if this assumption holds good. It will be satisfied only by a primary wave formation, i.e., by vertically accelerated motions, which, in my opinion, must not be neglected even in a first approximation. This will perhaps come about in such manner, that as a result of the horizontal oscillation of the ship-like wall of the oscillating body, local elevations and depressions of the surface occur which may take the form of spray.

In closing, I should like to say a word in favor of the expression “covibrating water mass” (mitschwingende Wassermasse). The lecturer, to be sure, has demonstrated quite correctly that the phenomena investigated are produced by hydrodynamic pressures which act on the surfaces of bodies in nonuniform motion. He accordingly recommends that the designation “covibrating mass” no longer be used. There exists, however, a cause-and-effect relationship between these pressures and the physical phenomenon in that throughout the entire field of the surrounding fluid particles of water must likewise be accelerated. These particles are accelerated with larger or smaller amplitudes, according to the distance from or the location

of the particles with respect to the disturbance created by the body. This, obviously, is the only basis on which we can explain the fact that the total effect of the hydrodynamic pressures can be described so clearly by the simple concept of an apparent increase in the mass or moment of inertia of the body which is independent of frequency. Naturally, it must be kept in mind that the concept of a limited mass of water taking full part in the ship motion is purely fictitious. For this reason, it is also referred to as a "reduced covibrating water mass."

Professor H. Ebner, Dr. Eng., Hamburg

1. Hydrodynamic masses and moments of inertia of ship theory also play a role for ships making turns as mentioned by Dr. Wendel in his discussion. In the case of the steady motion of a ship in a turning circle, the centrifugal force is not only influenced by the mass of the ship, but also by the "mass of water accelerated by the ship's motion." In this connection it should be noted, however, that the accelerated water mass in contrast to the mass of the ship has a direction associated with it and therefore, since the centrifugal force arises from the rotation of the momentum vector which acts in the longitudinal direction, it is the accelerated water mass for the longitudinal and not the transverse direction which is to be considered. As in the dynamics of rigid bodies, the motion of bodies moving in the water or on the surface can be determined from the general equations of motion of the dynamic system consisting of the body and the fluid set into motion. These equations differ from the usual fundamental dynamic equations only by the addition of the vector product of the velocity vector and the momentum vector which have different directions.

2. Some time ago, in order to clear up the question of how to determine the masses of water near a free surface which are accelerated by the lateral motions of floating bodies, we performed experiments in which the bodies were set into vibration about a longitudinal axis which lay above the water surface. The three models used had semi-circular, rectangular, and triangular cross sections. It was found that to obtain a center of rotation which agreed with experiment, the ratio of the accelerated water mass of the floating body to that of the body completed by reflection in the surface, i.e., the fully submerged body, is about 0.50 for the circle and rectangle but 0.85 for the triangle. The differences between these values and those obtained on the basis of the potential theory probably arise from the formation of the surface waves.

3. In the case of unsteady motion of bodies in water, it is necessary to add to the impulsive pressures arising from accelerated water mass, buoyant forces for which quasi-stationary assumptions will usually be made.

For the two-dimensional plate we can replace the quasi-stationary assumptions by exact ones in the form of unsteady circulation forces arising from the shedding of vortices. In the same way the stability and course of the unsteady motion in water of bodies behaving like plates can be determined. Further details are contained in an unpublished paper.

Ministerialrat (ret.) O. Schlichting, Berlin

The ideas presented by the lecturer were on a high plane which is not easily accessible to the practical shipbuilder and constructor. For this reason I may be permitted to warn against a conclusion which might be drawn from a statement contained in the paper to the effect that the hydrodynamic mass of the water accelerated by the bilge keels in rolling motions is the same, no matter whether the ship is underway or not. The stabilizing effect of the bilge keels on rolling motions is governed not only by the hydrodynamic mass but also by the speed of advance. This effect, which is probably evident by intuition and has been discussed in the Transactions of Naval Architects, is considerably greater for a ship underway than at rest.

Professor F. Horn, Dr. Eng. h.c., and Dr. Eng., Berlin

The paper of Dr. Wendel represents an excerpt from his comprehensive doctoral dissertation which was written about eight years ago. The complete text, which will be published later in our annual publication, places considerably higher demands on the theoretical knowledge of the reader than the excerpt presented here would indicate. It contains, as a matter of fact, a distinctly elegant theory. That this theory is nevertheless truly down to earth can be seen from the fact that results obtained on purely theoretical grounds are in most cases in very good agreement with experimental results, as demonstrated by the lecturer in several examples. In addition, however, it should also be noted here that we are dealing with a theory which is of great practical importance especially as applied to oscillation phenomena which are greatly influenced by the hydrodynamic masses and moments of inertia. Although the comprehension of this influence has already become widespread in the application to heaving and pitching oscillations as well as to elastic vibrations, there are much greater difficulties for the case of rolling oscillations where the particular hull shape must be considered to some degree. It is in this particular direction that the work of Dr. Wendel opens a promising avenue of advancement. It would be very desirable if the lecturer could, after the lapse of so many years, resume again and complete the calculations which he intended to carry out at that time and which would enable a comparison to be drawn with available test results.

I am very happy that the very valuable dissertation of Dr. Wendel which treats this important subject in the field of naval architecture in a coherent and systematic form for the first time and thereby fills a gap that has been widely felt until now, will soon be published in the Jahrbuch der Schiffbautechnischen Gesellschaft and will thus be made accessible to the profession at large.

Eng. F. Judaschke, Hamburg (submitted in writing)

In his investigations, Dr. Wendel justly emphasizes the point about which the ship rotates in its motions which are produced by the oncoming flow of the water. This point varies

in each case according to the load condition of the ship, i.e., the displacement curve and the weight curve change and thereby alter the character of the ship.

I cite a case from my own experience which deals with this problem. Approximately a year and a half ago, the ship "Wasserschutzpolizei 26" was remodeled in such a way that the boiler feed water which had previously been carried at the bottom of the ship was now stored on the sides of the ship alongside the lateral coal bunkers; in addition, the ship was provided with bilge keels. Both of these changes henceforth gave stability to the previously unsteady motions of the ship. For one thing, by removing the boiler water which had been moving about more or less freely at the bottom and by putting it into elevated tanks, the center of gravity was fixed to greater advantage. On the other hand, the bilge keel exerted its beneficial effect in turning maneuvers and in pulling alongside other ships. The ship, 24 m long, was of slender form and it had a relatively large top weight since it had previously been used by the Hydraulic Engineering Department as an inspection service craft. After remodeling it proved to be very useful to the harbor protection police operating on the broad Elbe River until it was finally destroyed during an air raid.

Closing Remarks by Dr. Wendel

Professor Dickmann presumes that in the case of transverse motion at the surface (see Figure 45), the hydrodynamic pressures do not show a sharp decrease in the direction of the surface. As a result of this, the hydrodynamic mass should also have approximately the same magnitude as it would in the case of the reflected double body, and not $1/3$ of this magnitude, as my own calculations indicate. Professor Dickmann has here hit upon the one particular result among those I calculated theoretically which, more than any other, needs to be verified by experiment. At the conclusion of my calculations in 1942, I immediately set up a testing program which, unfortunately, could not be carried out due to the unfavorable conditions of the time. Simple horizontal oscillation tests are presently being made with a beam at the Research Laboratory for Naval Construction of the Hamburg School of Engineering. The beam is being investigated deep under the surface, in air and at various intermediate positions, including a position at the surface. As far as the first tests indicate, there actually occurs a very great decrease in the hydrodynamic mass for the case of partial submergence. This is in agreement with my own values determined theoretically. The above-mentioned tests, once they are completed, will be published in the journal "Hansa."

The term "hydrodynamic mass" did not come to my mind until it was time to find a title for my investigations. To avoid speaking of "covibrating moments of inertia" and to avoid colorless expressions as far as possible, it does not seem far-fetched to use the terms "hydrodynamic mass" along with "hydrodynamic moment of inertia." Since I did not wish to revise the existing nomenclature, I myself have used both terms, "hydrodynamic mass" and "covibrating mass," side by side. The covibrating mass is to be introduced in the case of all types of accelerated and decelerated motions, even if we are not dealing with oscillations.

In the latter case, one would probably speak of "comoving mass" (mitbewegte Masse), but this expression can easily lead to misunderstandings.

The expression "covibrating mass of water" incidentally is only found in naval architecture and it presumably originated in the fundamental works of W. Froude and Kriloff. Quoting from these authors, we find:

W. Froude, "On the Rolling of Ships," Transactions Institute of Naval Architects (1861), page 188:

"And indeed if the mutual relations of the body of a ship and the contiguous masses of water be duly considered, it is sufficiently obvious that such a difference (between the period of a round-section vessel and the period of a ship with a sharp bottom and a very deep keel, Wendel) must arise in ships of such form; because independently of the resistance which the form must offer to the freedom of oscillation, we see that the resisting areas must put in motion large masses of water which will continue to accompany them inertly, as if forming part of the body of the ship herself."

A. Kriloff, "A General Theory of the Oscillations of a Ship on Waves," Transactions Institute of Naval Architects (1898), page 173:

"The moment A thus obtained, is the moment of inertia of the ship, together with that mass of water which takes part in her motion, making, so to say, a single body with her."

It is hardly likely therefore that the line of reasoning expressed by Professor Dickmann, which is in complete harmony with my own ideas as set forth in my paper, contributed in any way to the origin of the concept and expression "covibrating mass of water."

The statements made by Professor Ebner in regard to a ship's motion in turning incidentally confirm the fact that it is quite important to form a clear picture of the actual nature of the covibrating masses. These statements are very important for the investigation of the maneuvering of ships and it is to be hoped that he will soon publish them in more detailed form, suitable for practical application in naval construction. Point 2 has already been discussed above. I do not believe that free-oscillation tests, designed to determine the center of rotation, are the simplest and most reliable way to verify the theoretically obtained values for the hydrodynamic mass in the case of horizontal motion.

The statement made by Ministerialrat (ret.) Schlichting has really nothing to do with the subject under discussion. The forward motion of the ship indeed exerts a great influence upon the damping, i.e., the energy-dissipating effect of the bilge keels, but not on the increase in the moment of inertia to be introduced into the oscillation equation.

I should like to express my appreciation also to the other speakers who contributed to the discussion, among them especially Professor Horn, and to thank them for the interest taken in my lecture. Professor Horn recognized at once that it would be a very useful contribution to ship theory if the problems discussed were made the subject of a thoroughgoing investigation. At the suggestion of Professor Horn, the determination of the hydrodynamic mass and of the hydrodynamic moment of inertia of an actual ship was carried out according to the method

indicated in Parts II, III, and IV. This work, which was already in an advanced state of completion, was destroyed when the Institute of Technology in Charlottenburg was devastated during the war.

Professor G. Schnadel, Dr. Eng., Hamburg

Dr. Wendel has discussed an important field of ship theory. The problem presented by the lecturer reaches back very far; it goes back to the establishment of the first formulas which Otto Schlick set up for the vibration of ship hulls in 1884. It is particularly important that the calculation of the reduced mass of water which has a decisive influence on the oscillations has now been definitely cleared up. Nevertheless, I should like to point out one more thing:

The role of the water mass influenced by the oscillation has been previously treated by Koch, *Ingenieur-Archiv* 1933, Vol. 4, page 103. Koch determined the effect experimentally with the aid of the electrical analogue and has drawn up graphs of the results.

I myself used Koch's investigations later on for the determination of elastic oscillations in connection with the launching of the "Caribia" (see *Jahrb. d. STG.*, Vol. 35, 1935, page 87).

It is very gratifying to know that Dr. Wendel has now succeeded in carrying out the mathematical determination of the hydrodynamic masses for a limited depth of water which had been determined experimentally by Koch.

I should like to express my very keen appreciation to Dr. Wendel on my own behalf and also in the name of the *Schiffbautechnische Gesellschaft* for his interesting exposition.

INITIAL DISTRIBUTION

Copies

12 Chief, BuShips, Library (Code 312)
 5 Tech Library
 1 Tech Asst to Chief (Code 106)
 1 Appl Science (Code 370)
 1 Noise, Shock, & Vibra (Code 371)
 for Mr. E.F. Noonan
 1 Ship Design (Code 410)
 1 Prelim Des & Ship Protec (Code 420)
 1 Submarines (Code 525)
 1 Propellers & Shafting (Code 554)

3 CHBUORD, Underwater Ord (Re6a)

3 CHBUAER
 2 Aero & Hydro Br (AD-3)
 1 Appl Math Br (RS-7)

4 CHONR
 1 Math (432)
 2 Mech (438)
 1 Undersea Warfare (466)

2 OPNAV, OP 922F2

2 DIR, USNRL

4 CDR, USNOL, Mech Div

1 CDR, USNOTS, Inyokern, Calif.

1 CDR, USNOTS, Underwater Ord Div,
 Pasadena, Calif.

2 CDR, Portsmouth Naval Shipyard
 1 Scientific & Test Br (Code 251)

1 CDR, Mare Island Naval Shipyard

1 CDR, Norfolk Naval Shipyard

2 CO, USNUOS, Newport, R.I.

1 DIR, Marine Physical Lab, USNEL,
 San Diego, Calif.

2 DIR of Aero Res, NACA

2 DIR, Langley Aero Lab, Langley Field, Va.

2 DIR, Lewis Fl Propulsion Lab, Cleveland, O.

2 DIR, Ames Aero Lab, Moffett Field, Calif.

2 CO, Arnold Engin Dev Ctr, Tullahoma, Tenn.
 1 Gas Dynamics Facility

Copies

1 CG, Aberdeen Proving Ground, Aberdeen, Md.
 Attn: Ballistics Res Lab

1 DIR, Oak Ridge Natl Lab, Oak Ridge, Tenn.

2 DIR, Natl BuStand
 1 Hydraulic Lab

2 ASTIA, Document Service Ctr, Dayton, O.
 Attn: Service Div

1 Bureau of Reclamation, Denver Fed Ctr,
 Denver, Colo. Attn: Tech Ref Section

1 DIR, U.S. Waterways Expmt Stn, Vicksburg, Miss.

1 Resident Member, Beach Erosion Bd

1 CO, Frankford Arsenal Office of Air Res,
 Appl Mech Grp, Wright-Patterson AFB, O.

1 DIR, Appl Physics Div, Sandia Lab, Sandia
 Base, Albuquerque, N.Mex.

1 Chief, Hydraulic Data Br, TVA, Knoxville, Tenn.

1 Editor, Bibliography of Tech Rpts, Office of
 Tech Services, US Dept of Commerce

1 Editor, Aero Engin Rev, New York, N.Y.

1 Editor, Appl Mech Rev, Southwest Res Inst,
 San Antonio, Tex.

2 The John Crerar Library, Chicago, Ill.

1 Mr. Barton B. Cook, Jr., DeLaval Steam Turbine
 Co, Trenton, N.J.

1 Mr. Thomas Frink, Glenn L. Martin Co,
 Mail No. 383-B, Baltimore, Md.

1 Mr. Vito L. Russo, Div of Ship Des, Maritime
 Admin, US Dept of Commerce

MIT LIBRARIES



3 9080 02993 0564

MAR 24 1981

FEB 22 1983